

# An Analysis of the Gel Point of Polymer Model Networks by Computer Simulations

M. Lang, T. Müller\*

*Leibniz Institut für Polymerforschung Dresden, Hohe Straße 6, 01069 Dresden, Germany*

E-mail: lang@ipfdd.de

## Abstract

The gel point of end-linked model networks is determined from computer simulation data. It is shown that the difference between the true gel point conversion,  $p_c$ , and the ideal mean field prediction for the gel point,  $p_{c,id}$ , is a function of the average number of cross-links per pervaded volume of a network strand,  $P$ , and thus, contains an explicit dependence on junction functionality  $f$ . On the contrary, the amount of intra-molecular reactions at the gel point is independent of  $f$  in a first approximation and exhibits a different power law dependence on the overlap number of elastic strands as compared to the gel point delay  $p_c - p_{c,id}$ . Therefore,  $p_c - p_{c,id}$  cannot be predicted from intra-molecular reactions and vice versa in contrast to a long standing proposal in literature. Instead, the main contribution to  $p_c - p_{c,id}$  for  $P > 1$  arises from the extra bonds (XB) needed to bridge the gaps between giant molecules separated in space and scales roughly  $\propto (P - 1)^{-1/2}$ . Further corrections to scaling are due to non-ideal reaction kinetics, composition fluctuations, and incompletely screened excluded volume, which are discussed briefly.

# Introduction

Polymer networks and gels are materials that have reached a wide range of applications ranging from car tyres to drug delivery, removal of pollutants, artificial muscles, or stretchable electronics<sup>1-4</sup>. One point of major interest for theory, processing and application is the exact location of the gel point<sup>5,6</sup>, since there, the reacting liquid turns into a solid. The properties next to the gel point are well understood for critical percolation and mean field models as a function of the distance to the gel point. The prediction of the percolation threshold or the gel point itself remains a challenging problem for theorists<sup>7-10</sup>. Typically, the classical Flory-Stockmayer (FS) theory<sup>11,12</sup> or an equivalent mean field model<sup>13,14</sup> is taken for a first estimate based upon an ideal system whereby both intra-molecular reactions prior to gelation and the positions of the reacting molecules in space are neglected. Previous generalizations of the FS theory<sup>6,15-22</sup> focus essentially on corrections due to intra-molecular reactions (“loops”), since the self-contacts of random walks or branched polymers in semi-dilute solutions are well understood. The impact of the spatial arrangement of the reacting molecules on the position of the gel point was essentially ignored in literature due to the lack of an analytical approach that allows for a quantitative treatment of this point.

One remarkable result of these models (mean field + loop correction) is that the latest variant of it<sup>22</sup> seems to work even for overlap numbers around one and below, which is in the core of the critical percolation regime or even requires diffusion of the molecules to allow for network formation. On the contrary, there is a number of simulation works<sup>23-28</sup> (see section “Numerical studies in literature” of the Appendix for a more detailed discussion) that indicate that the loop correction might not be sufficient to explain the delay of the gel point for overlap numbers clearly above one. These works, however, could be criticized, since network formation was modeled either without diffusion of the reactive species<sup>23-26</sup>, or analyzed only indirectly<sup>27</sup>, or some inconsistency among the data is apparent<sup>28</sup>. Nevertheless, the simulation studies<sup>23-28</sup> are in line with the scaling model of percolation, where the hyperscaling relation connects the fractal dimension of the branched molecules to space dimension<sup>8</sup>: extra

reactions are necessary to bridge the gaps between the separated giant molecules just below the gel point. This is not accounted for in the mean field models. It should be observable as a gap between the conversion at the true gel point and a mean field estimate for the gel point were corrections due to intra-molecular reactions were considered.

Using the jargon of percolation, the gelation of  $f$ -functional stars (GS) - or equivalently, the end-linking of  $N$ -mers through  $f$  functional junctions - is a non-nearest neighbor percolation problem of almost randomly distributed sites with limited “valence” (the junction functionality  $f$ ). Originally, any kind of non-nearest neighbor percolation problems was termed “long-range percolation”<sup>29-34</sup>. This nomenclature has partially changed in recent years, since a distinction among qualitatively different “long-range” models could be made. The general finding is that an exponential cut-off or a hard range limit for the bonds maintains a window of critical percolation next to the critical point. However, the range of conversion where critical percolation can be observed might be rather narrow, if a large number of neighbors can be reached<sup>35</sup>. Therefore, it was speculated that the narrow range of conversions with critical properties may not be accessible experimentally<sup>31</sup>. This motivated to estimate the gel point delay by mean field arguments, also, since it was shown that the size distribution of the smallest loops near the gel point follows mean field statistics<sup>22,36</sup>.

Nevertheless, GS falls within this class of “short-range” problems, since the end-to-end distribution of the bonds (the polymer strands) is characterized by an exponential decay. Power law decays for the bond length distribution can lead to a short range behavior, to a small-world behavior for a certain window of power laws depending on space dimension, or to a true long-range behavior, which is mean-field like on all scales<sup>37,38</sup>. A limited valence of the nodes has no effect<sup>39,40</sup> on the critical behavior once  $f \geq 3$ , but affects certainly the location of the critical point. Thus, the general applicability of percolation to model GS in the vicinity of the gel point is out of question and has been corroborated by more recent works on percolation within a range<sup>41-43</sup> (some newer works call this type of problems “medium-range percolation”<sup>43</sup> or “equivalent neighbor percolation”<sup>41</sup>).

Nevertheless, there are several points that are different in GS as compared to the percolation problems that were studied previously:

1. Reactions between molecules occur based upon a diffusion reaction mechanism. The applicability of critical percolation approximation requires that diffusion effects are not important.
2. The position of network junctions couples to the local polymer density once these become connected to chains. Composition fluctuations arise for cross-linking at the presence of a solvent or if different chemical species are linked together to form a network (e.g. chains and junctions). These composition/interaction effects can introduce a second characteristic length scale that may affect the scaling in the vicinity of the gel point.
3. The number of accessible junctions depends not only on range (here given by degree of polymerization, chain stiffness, and solvent quality) but also on the junction functionality, polymer volume fraction, and the stoichiometric ratio  $r$  of reactive groups on junctions vs. reactive groups on chains.

Indeed, kinetic gelation is one example where the diffusion reaction mechanism dominates the behavior and causes a different universality class as compared to critical percolation<sup>44</sup>. Similarly, diffusion limited cluster aggregation is a different universality class<sup>45</sup> and would become relevant once the overlap number of stars drops below one. For sufficiently large overlap numbers it is expected that diffusion becomes unimportant in the close vicinity of the gel point, since the behavior of the system is dominated there by the largest molecules, which diffuse extremely slow because of the high viscosity next to the gel point. What is not accounted for in this discussion is that the local dynamics and accessibility of the nodes depends on the number of attached chains. Thus, bonds are no more inserted randomly into the system, instead, nodes with a smaller number of existing connections exhibit a higher

rate of bond formation. We analyze this point in the appendix and correct the mean field estimate for the critical point accordingly.

The second point above is suppressed to a significant extent by analyzing network formation in good solvents or melts. Also, the homo-polymerization of stars instead of a co-polymerization of junctions and chains or stars of two different types is preferable here. In the best possible case (homo-polymerization of stars), the length scale at which the local concentration of the nodes couple to a constant polymer density is comparable to the size of the network strands and thus, irrelevant for the behavior in the vicinity of the gel point. Nevertheless, it is certainly of interest to analyze the impact of statistical fluctuations in composition in case of end-linking reactions, since end-linking reactions are the literature standard for gelation studies of model networks. This point is also of relevance for high conversions, since composition fluctuations freeze in during the cross-linking reaction<sup>46</sup>.

The third point is explained best when comparing the average number of possible neighbors  $P$  to which a node can connect in typical percolation studies with GS. In bond percolation where bonds are introduced within a range  $R$ , the number of neighbors  $P$  is typically a constant number of roughly  $P \approx \rho R^3$ , where  $\rho$  is the number density of nodes. On the other hand, the corresponding overlap number of junctions for the simplest case of GS homo-polymerization of monodisperse stars with  $N/f$  Kuhn segments per arm is given by

$$P \approx \frac{8\pi\phi R^3}{3fNb^3}. \quad (1)$$

Here,  $R$  is the average extension of the network strands that depends on the number of Kuhn segments,  $N$ , the root mean square size of a Kuhn segment,  $b$ , and the solvent quality.  $\phi$  is the polymer volume fraction and  $b^3$  a rough estimate for the occupied volume of a Kuhn segment. Thus,  $P$  is an explicit function of the valence  $f$  in case of polymer gelation in contrast to typical long range percolation studies, where the number of bonds can be up to  $\approx \rho R^3$ .

The above points and the question whether the gel point can be estimated by a consideration of intramolecular reactions is addressed with our publication. We simulate explicitly the dynamics, conformations, and reactions of the molecules that form the network in space to remove the limitations of previous simulation studies. We determine intra-molecular reactions and the position of the gel point. On this basis, we demonstrate that the delay of the gel point is not controlled by intra-molecular reactions. We show that the dominating contribution is due to extra bonds (XB) that are necessary to bridge the gaps between the giant molecules. We discuss corrections that arise due to a different mobility of the reacting species, due to composition fluctuations, and due to incompletely screened excluded volume. Furthermore, we provide examples how the delay of the gel point could be analyzed with more detail in the experiment.

## Computer Simulations

For our study, we use the Bond Fluctuation Model (BFM)<sup>47,48</sup>, which is a well known lattice based Monte-Carlo method that has been used frequently to simulate polymer model systems<sup>49–51</sup>, solutions<sup>52,53</sup>, membranes<sup>54</sup>, melts<sup>55,56</sup>, or networks<sup>57,58</sup>. In this simulation method, chains are represented by a connected set of small cubes that resemble the monomers of the chain. Monomers are connected into chains (and later: to network junctions) through a discrete set of 108 different bond vectors. Monodisperse melts made of  $M$  chains with a degree of polymerization  $N = 8, \dots, 64$  were equilibrated by random jumps of the monomers under the constraint that all bonds remain within the allowed set of bond vectors. All simulations were run on a lattice of  $256^3$  lattice sites with periodic boundaries. A stoichiometric amount of  $X = 2M/f$  network junctions are also modeled by small cubes and are added at random positions to the melt of chains such that approximately  $2^{20}$  monomers occupy a volume fraction of  $\phi \approx 0.5$  of the lattice sites, see Table 1 for the simulation parameters. This volume fraction is standard for the simulation of dense systems like melts or networks

using the BFM<sup>59,60</sup>.

After equilibration of the reaction mixture, end-linking reactions were turned on while chain monomers and junctions perform a stochastic motion inside the reaction bath. Whenever a free chain end was in one of the nearest neighbor positions to a junction that was not yet completely reacted, a bond was introduced between both. The chain end is then bound to the junction and the number of possible further reactions of the junction is reduced by one. 100 statistically independent samples (by initial positions of cross-links and chain conformations) with the same simulation parameters were created and subsequently linked into networks in order to improve statistics. Note that our simulations explicitly model a diffusion collision mechanism in space to simulate reactions. This is different to the random insertion of bonds either between spatially correlated neighbors as in percolation studies or only correlated within a single molecule as in recent mean field work<sup>22</sup>.

## Mean field estimates of the gel point

The ideal reference for the gel point of our end-linked model networks is<sup>14</sup>

$$p_{c,id} = \left( \frac{1}{f-1} \right)^{1/2} \quad (2)$$

and the delay of the gel point conversion with respect to  $p_{c,id}$  is quantified below as  $p_c - p_{c,id}$ . The power of 1/2 in the above equation results from the two bonds at both chain ends that are necessary to link the  $f$ -functional junctions.

intra-molecular reactions in the reaction bath are determined by counting the number of connected components,  $C$ , the total number of bonds,  $B$ , between initial molecules with a total number of  $M + X$ . Then, the cycle rank (total number of independent circuits in the graph)

$$\xi = B - (M + X) + C \quad (3)$$

provides the total number of intra-molecular reactions in the reaction bath<sup>61</sup>. It has been argued by several authors<sup>6,11,15-22</sup> that the formation of finite loops (intra-molecular reactions) controls the displacement of the gel point with respect to  $p_{c,id}$ , since each intra-molecular reaction diminishes the number of branching reactions by one. Thus, we estimate the shift of the gel point due to intra-molecular reactions,  $\Delta p$ , with respect to the total number of possible reactions,  $2M$ , through

$$\Delta p = \xi/(2M). \quad (4)$$

Then,

$$p_c - \Delta p(p_c) = p_{c,id} \quad (5)$$

provides a self-consistent mean field estimate for the gel point,  $p_c$ , that is corrected by intra-molecular reactions.

Below, we will see that such a self-consistent approach underestimates cyclization at the true gel point. Therefore, the  $\Delta p$  data in Table 1 were collected at the true gel point as determined by the onset of a non-vanishing modulus. The data for a self-consistent determination of  $\Delta p$  are included in Figure 4 for completeness and available with high accuracy through the fit of the corresponding data.

Each intra-molecular reaction creates a cyclic structure inside the network (“loop”). We have analyzed loop size distributions in section “intra-molecular reactions” of the Appendix. Our results show that the size distribution of loops is  $\propto i^{-5/2}$  in a good approximation next to the true gel point, where  $i$  is the number of precursor chains that establish the loop. In consequence, we expect that the total amount of loops at the gel point is independent of  $f$  up to minor corrections for smallest  $i$ , since a dependence  $\propto i^{-5/2}$  refers to a mean field gel point where there is in average exactly one path to the infinite gel in the limit of large  $i$  (see also equations (20) to (24) of Ref.<sup>36</sup> or equation (A2-44) of Ref.<sup>62</sup>). A mean field scaling for the short range statistics is expected for overlap numbers  $\geq 1$  and has been found previously in non-nearest neighbor bond percolation<sup>32,63</sup>.



Table 1: Simulation parameters and gel point estimates.  $f$  is the junction functionality,  $N$  the degree of polymerization of linear chains between junctions, and  $X$  is the total number of junctions per simulation. The gel point is estimated from simulation data in two different ways a) By an extrapolation of modulus data,  $p_{c,\mu}$ , with critical exponent  $\mu$  that is fit to the data, and b) by an analysis of the weight average degree of polymerization  $N_w$  as  $p_{c,\gamma}$  with an exponent  $\gamma$ .  $C_-/C_+$  is the ratio of the coefficients of the branches of  $N_w$  below and above the gel point. The conversion lost in intra-molecular reactions,  $\Delta p$ , is measured at  $p_{c,\mu}$ .  $p_d$  is the mean field estimate for the gel point that reflects unequal reactivity, while  $p_{c,id}$  assumes binomially distributed connections on junctions and chains. The standard deviation for  $p_d$  is below  $10^{-3}$ , the error for  $\Delta p$  is below  $3 \times 10^{-4}$  while the error for the determination of  $p_{c,\mu}$  is about  $10^{-3}$ . For  $p_{c,\gamma}$ , we require four digits behind the comma to fix the numerical optimum of a parallel decay of both branches, but the last digit is certainly not significant as visible from the large error for  $\gamma$  and the scatter of the  $N_w$  data.

$f$	$N$	$X$	$p_{c,\mu}$	$\mu$	$p_{c,\gamma}$	$\gamma$	$C_-/C_+$	$p_{c,id}$	$\Delta p$	$p_d$
3	8	80653	0.750	$1.78 \pm 0.01$	0.7506	$1.47 \pm 0.05$	$3.0 \pm 0.8$	0.7071	0.0213	0.690
3	16	41942	0.742	$1.81 \pm 0.01$	0.7409	$1.45 \pm 0.06$	$3.0 \pm 0.9$	0.7071	0.0145	0.695
3	32	21398	0.732	$1.81 \pm 0.01$	0.7344	$1.46 \pm 0.07$	$3.5 \pm 1.4$	0.7071	0.0100	0.700
3	64	10810	0.725	$1.90 \pm 0.02$	0.7272	$1.37 \pm 0.07$	$2.7 \pm 0.8$	0.7071	0.0070	0.697
4	8	61680	0.636	$1.74 \pm 0.01$	0.6371	$1.54 \pm 0.07$	$3.0 \pm 1.2$	0.5774	0.0225	0.562
4	16	31774	0.622	$1.80 \pm 0.01$	0.6230	$1.53 \pm 0.11$	$2.0 \pm 1.4$	0.5774	0.0153	0.568
4	32	16130	0.611	$1.86 \pm 0.02$	0.6135	$1.38 \pm 0.07$	$2.2 \pm 0.7$	0.5774	0.0106	0.568
4	64	8128	0.601	$1.88 \pm 0.02$	0.6041	$1.31 \pm 0.06$	$2.0 \pm 0.5$	0.5774	0.0073	0.569
6	8	41942	0.523	$1.69 \pm 0.02$	0.5235	$1.53 \pm 0.11$	$3.0 \pm 1.5$	0.4472	0.0239	0.436
6	16	21398	0.503	$1.89 \pm 0.02$	0.5043	$1.43 \pm 0.09$	$2.0 \pm 1.2$	0.4472	0.0161	0.442
6	32	10810	0.492	$1.78 \pm 0.02$	0.4916	$1.37 \pm 0.05$	$1.7 \pm 0.9$	0.4472	0.0112	0.444
6	64	5433	0.481	$1.95 \pm 0.04$	0.4813	$1.28 \pm 0.05$	$1.8 \pm 0.4$	0.4472	0.0077	0.442

A rough estimate of the generation  $i$  at which a cross-over to critical percolation is expected can be made through the Ginzburg criterion. Let us introduce the relative extent of reaction,

$$\epsilon = (p - p_c) / p_c, \quad (6)$$

as a measure of conversion  $p$  with respect to the conversion at the true gel point,  $p_c$ . According to experimental data<sup>64</sup> for  $f = 4$  (same  $f$  as in Figure 8), the value of  $\epsilon$  at the cross-over to critical percolation,  $\epsilon_G$ , is  $\epsilon_G \approx N^{-1/3}/10$ , which provides  $\epsilon_G \approx 1/20$  for the data of Figure 8. We expect mean field scaling up to this average number of strands  $i \approx 20$ . The amount of loops in generations  $i \geq 20$  contributes only a minute portion to the total number of loops in the range of 1-2% depending on whether mean field or critical scaling is assumed for the loop size distribution. Thus, the total amount of intra-molecular reactions is rather accurately estimated by adopting a mean field model for the loop size distribution in the vicinity of the gel point. We further note that our simulation results for  $\Delta p$  represent formally an upper bound for macroscopic systems, since a minute part of cyclic structures is closed through the periodic boundary conditions (finite size effect). These artificial giant loops involve of order  $L^2/b^2 \approx 10^4$  segments and thus, loops with  $i \gtrsim 10^4/N$  chains, which yields a contribution to  $\Delta p$  below the statistical error. Therefore, finite size corrections can be ignored for  $\Delta p$ .

In a more general form, the width of the percolation regime  $|p - p_c|/p_c$  for long range percolation can be estimated<sup>35</sup> as a function of the number of possible reaction partners  $P$

$$\epsilon_G \cong P^{-2/(6-d)}. \quad (7)$$

The width of the critical zone refers to a relative extent of reaction in the range of (after dropping coefficients of order unity and using equation (1))

$$\left| \frac{p - p_c}{p_c} \right| \lesssim \left( \frac{f}{\phi N^{1/2}} \right)^{2/3}. \quad (8)$$

This leads to the well known result of  $\epsilon_G \propto N^{-1/3}$  for melts with  $\phi = 1$  and  $R \approx bN^{1/2}$ , but indicates also that  $\epsilon_G \propto f^{2/3}$ .

A second possible deviation from mean field results from a different mobility and accessibility of junctions (and eventually chain ends) as a function of the number of existing connections to other molecules. In similar manner, concentration fluctuations of junctions and chain ends may affect the distribution of connections of the molecules. In consequence, this connectivity distribution is no more a binomial one, which we indeed observe in our simulations, see section “Unequal reactivity” of the Appendix. This difference to the ideal case can be considered within a mean field approach by mapping the system to a co-polymerization of junctions and chains with functionality distributions that equal the distribution of the number of connections at a given conversion  $p$  as described in more detail in the Appendix. Let  $f_e$  denote the weight average number of connections among the junctions and  $g_e$  the weight average number of connections of chains. Then, the gel point reflecting the non-ideal distribution of connections is<sup>13</sup> the conversion  $p_d$  where  $(f_e - 1)(g_e - 1) = 1$  for the stoichiometric systems of our study. This condition is determined numerically from the simulation data and given in Table 1. The corresponding mean field estimate for the gel point that reflects both non-ideal reactivity and intra-molecular reactions is given in good approximation by  $p_d + \Delta p$ , see Table 1.

For all networks of our study, the impact of lower accessibility and mobility of junctions causes a smaller  $f_e$  next to the gel point as compared to the binomial reference case. On the contrary,  $g_e$  seems to be dominated by concentration fluctuations as the portion of chains with two connections increases quicker than  $p^2$ . In total, most of these two competing corrections compensates each other and causes only a small shift of the estimated gel point towards lower conversions,  $p_d < p_{c,id}$ . Thus,  $p_{c,id} + \Delta p$  is an upper bound for a mean field estimate with corrections due to intra-molecular reactions. This observation holds for all samples of our study and indicates that composition fluctuations are more relevant than mobility or accessibility of the reactive groups, at least for the low  $f \leq 6$  of our study. Furthermore,

we have to point out that our simulations were performed in the diffusion controlled regime where the impact of mobility is expected to be largest. Experiments are typically reaction controlled. Thus, a quantitatively larger shift of  $p_d$  towards lower conversion can be expected, in particular, since our simulations refer also to the limiting case of a perfect mixture. Based upon this observation, we recommend that experimental tests of theory should be conducted with a homo-polymerization of  $f$ -functional stars as model systems, since this architecture diminishes the impact of a different mobility as only chain ends react. Also, concentration fluctuations of reactive groups are suppressed to a length scale comparable to the size of the stars, if reactions are conducted in a sufficiently good solvent or in melt.

## Gel point estimate based upon phantom modulus

The gel point can be determined from the onset of a non-vanishing equilibrium modulus of the networks. In the vicinity of the gel point, the phantom contribution to modulus dominates the elasticity<sup>65</sup>. We analyze the phantom modulus as suggested in Ref.<sup>66</sup> by considering that each chain is an ideal elastic spring of stiffness  $\propto N^{-1}$ . This direct determination is preferable as compared to counting the cycle rank, since the elastic contribution of a network cycle depends on its size and embedding into the network structure<sup>67-70</sup>: network strands in small loops (by number of strands) contribute in average less to modulus than strands in large loops. The classical limit is reached for loops made of an infinite number of strands (infinite tree approximation). The origin for this difference is that the extension of a strand of  $N$  segments within a cyclic polymer of  $iN$  segments is in average smaller than in its linear counterpart. Since modulus is the free energy change with respect to elongation, it is the time average size of the strands that determines the contribution to modulus (and not only network connectivity as assumed when considering the cycle rank)<sup>68,70</sup>. Qualitatively, this behavior is somewhat similar to the behavior of de-swollen gels<sup>71</sup> where the reduced chain extension in the dry state causes a significant reduction of modulus as compared to gels that

were prepared in the dry state.

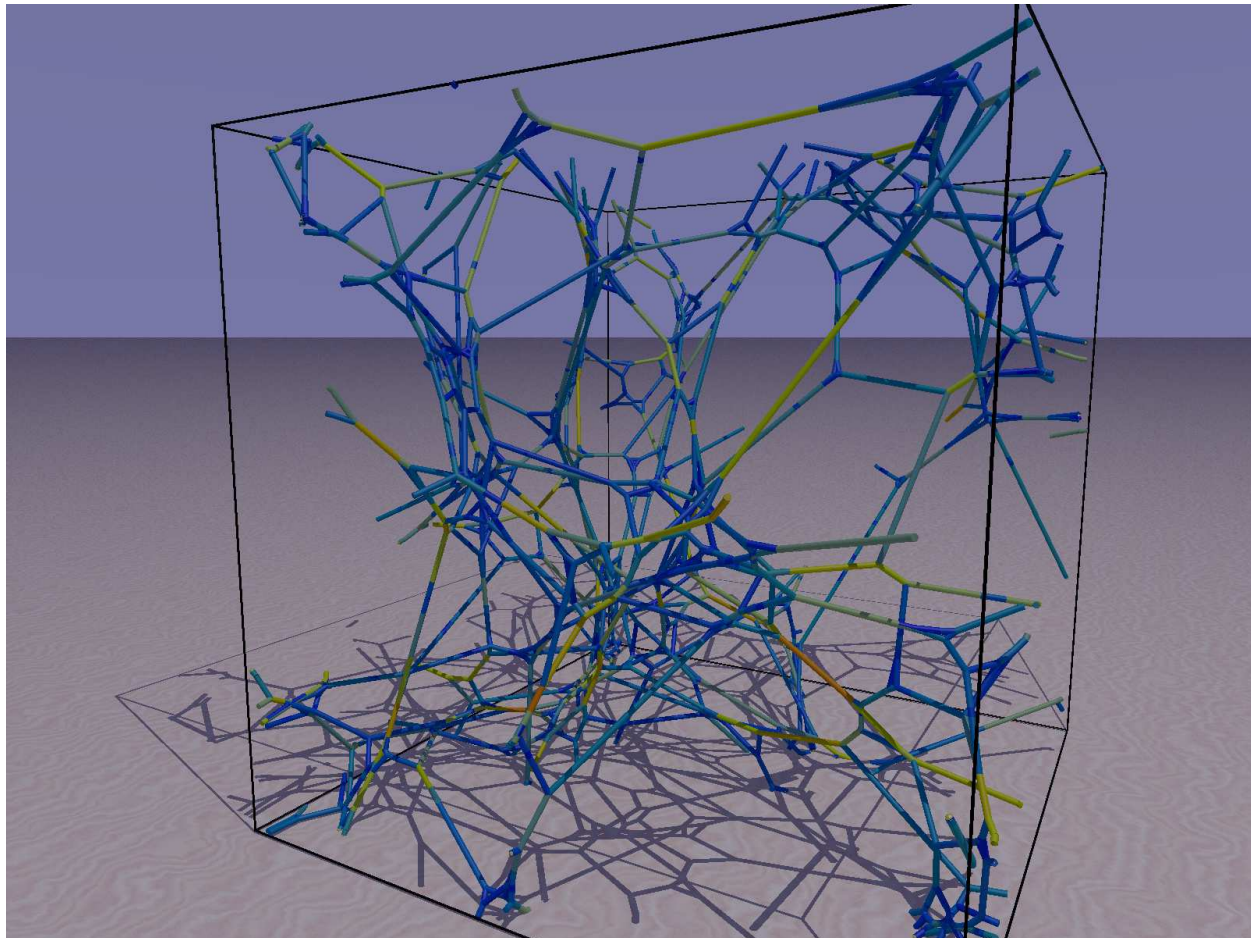


Figure 1: The force balance condition for the determination of the phantom modulus of a network with  $f = 4$  and  $N = 8$  is shown at  $p = 0.67$  not far beyond the gel point. The color code (from blue to red) corresponds to a different strain of the strands. Note that only the elastically active material is shown and that single strands between branch points correspond typically to a sequence of several linear chains or loops, since  $p$  is close to the gel point. A change in color along one straight connection indicates, therefore, a change in topology (for instance, a linear strand followed by a stretched loop where the loop strands carry less load, etc ...).

For a network of ideal springs, the ground state is determined numerically by considering a simultaneous force balance at all junctions. Below, the gel point, the ground state refers to a collapse of the structure into a single point. Above the gel point, the periodic boundaries of the sample prevent this collapse and a non-zero size of the springs is obtained. An example for the force balance condition to determine modulus is shown in Figure 1 for a network with

parameters  $f = 4$  and  $N = 8$  at  $p = 0.67$ . Finally, the resulting elastic energy density within the samples is averaged over the 100 copies of equivalent networks to determine the average phantom modulus of the samples.

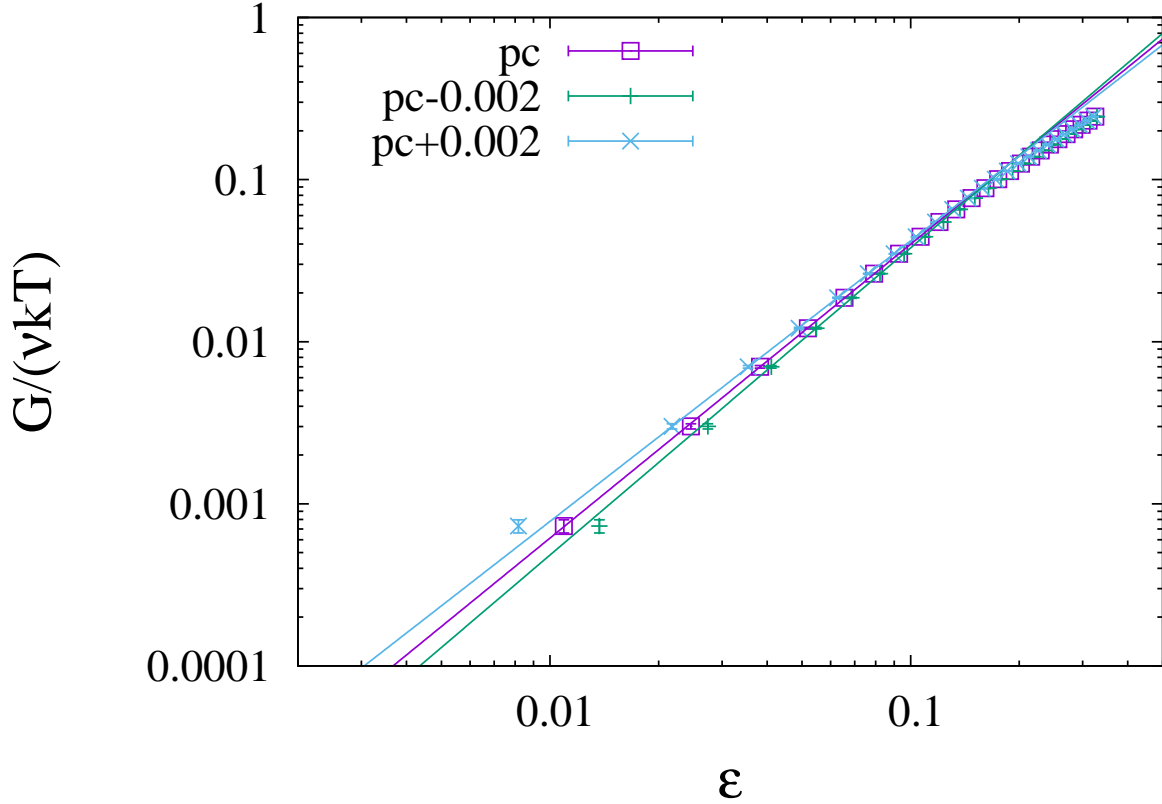


Figure 2: Scaling of phantom modulus in the vicinity of the gel point for the networks with  $f = 3$  and  $N = 32$ . A presumed  $p_{c,\mu}$  that is either 0.002 below or above the optimum  $p_c$  already leads to significant deviations (beyond error bar) from a power law dependence for the smallest  $G$  values.

In the scaling model of gelation, it is expected that phantom modulus grows in the vicinity of the gel point as a power law

$$G \propto \epsilon^\mu. \quad (9)$$

In order to detect the gel point, we vary  $p_c$  in steps of  $10^{-3}$  and fit all data with a modulus in the range  $10^{-4}G_{\max} < G < G_{\max}/20$  to a power law  $\epsilon^\mu$ . Here,  $G_{\max}$  is the maximum modulus at maximum conversion. The boundaries for the fit serve to reduce noise effects at the lower

bound and to exclude the cross-over to mean field at large  $G$ . The gel point is identified as the conversion with the lowest deviation to a power law dependence in the above range with focus on smallest  $G$  values and denoted below as  $p_{c,\mu}$ . Typically, a clear power law dependence over one and a half decades is found for the smallest  $G$  values for a narrow range of conversions with a width of approximately  $10^{-3}$  around the “gel point”. Figure 2 shows a typical example for the detection of this  $p_{c,\mu}$  plus two examples with a slightly deviating estimate for the gel point. The exponent  $\mu$  is taken as an adjustable parameter and fit to the data. The results of these fits for  $p_{c,\mu}$  and  $\mu$  are summarized in Table 1.

For mean field,  $\mu = 3$  is expected<sup>72</sup> in agreement with scaling predictions for 6 dimensions. For critical percolation, one expects for  $d = 3$  according to<sup>73-75</sup>  $\mu = \zeta + \nu(d - 2)$  that there is approximately  $\mu \approx 1.9$ . Estimates for the exponent  $\nu$  that describes the divergence of the correlation length were originally<sup>76</sup> about  $\nu \approx 0.9$ , while more recent renormalization group estimates or simulation data provide slightly lower values of  $\nu \approx 0.82$  or  $\nu \approx 0.875$  respectively<sup>77</sup>. The exponent  $\zeta$  describes the divergence of the resistance of the links when approaching the gel point. It was previously assumed<sup>74,78</sup> that  $\zeta$  is close to one for  $d = 3$ , which has been confirmed by more recent renormalization group estimates that yield<sup>77</sup>  $\zeta \approx 1.05$  and by numerical data<sup>79</sup> with  $\zeta \approx 1.117 \pm 0.019$ . Literature values of experimental or simulation data for  $\mu$  are largely scattered in the range of<sup>76,78</sup>  $1.4 \leq \mu \leq 2.45$ . Our results for  $\mu$  range from 1.69 to 1.95 with an average of  $1.82 \pm 0.03$ , which is in rather good agreement with critical percolation, in particular with renormalization group estimates for all contributing exponents, which yield  $\mu \approx 1.87$ .

The positions of the gel points are all well above the estimates based upon intra-molecular reactions,  $p_{c,\mu} > p_{c,id} + \Delta p$ , and do not agree with these within the error of the analysis. Note also that gel points like  $p_{c,\mu}$  are underestimated systematically in finite samples as shown, for instance, in Figure 1 of<sup>78</sup>. Therefore, our results for  $p_{c,\mu}$  are lower bounds for the gel points of macroscopic samples. Since finite size effects can cause only a systematic enlargement of  $\Delta p$  (extra loops through periodic bounds, see the preceding section), also the observed gaps

between  $p_{c,\mu}$  and  $p_{c,\text{id}} + \Delta p$  are lower bounds for the equivalent data of macroscopic samples.

## Gel point estimated based upon weight average molecular weight

As a second estimate for the gel point, we analyze the weight average degree of polymerization of the soluble molecules,  $N_w$ . Theoretically, a dependence of

$$N_w \propto |\epsilon|^{-\gamma} \quad (10)$$

is expected, with best estimates for the exponent of  $\gamma \approx 1.82 \pm 0.04$  (3rd order  $\epsilon$  expansion<sup>80</sup>),  $\gamma = 1.805 \pm 0.02$  (from series expansion of the cluster size distribution<sup>81</sup>), or  $\gamma = 1.795 \pm 0.005$  (Monte-Carlo data by R. M. Ziff and G. Stell<sup>77,81,82</sup>). Experimental data fits to exponents in the range of<sup>76</sup>  $1.63 \leq \gamma \leq 1.91$ . For mean field, the corresponding exponent is  $\gamma = 1$ .

The gel point estimate  $p_{c,\gamma}$  and exponent  $\gamma$  is determined from  $N_w$  data as suggested in Refs.<sup>44,83,84</sup>: we plot simultaneously the reduced  $N_w(p)$  (excluding the largest cluster<sup>22,23,44,58,85,86</sup>) above  $p_c$  and the total  $N_w(p)$  below  $p_c$  as a function of  $|\epsilon|$  and shift  $p_c$  such that the steepest decay<sup>1</sup> of both branches shows the same slope. The resulting estimate for  $p_c$  is denoted by  $p_{c,\gamma}$  for a better distinction from other estimates and summarized in Table 1. The exponent  $\gamma$  including the error estimate from the fit is given also in Table 1.  $p_{c,\gamma}$  had to be adjusted with four digits accuracy to achieve parallel upper and lower branches of  $N_w(p)$ , however, there is typically less than one order of magnitude in  $|\epsilon|$  where the  $N_w$  data appears to be linear on a log-log plot, see Figure 3 for the “worst case” example where  $\gamma$  deviates most from the prediction of critical percolation. In comparison, the modulus data is linear on a log-log plot for typically one and a half decades. Therefore, we expect that  $p_{c,\mu}$  should be

---

<sup>1</sup>For our simulations, there is a cross-over to mean field at large  $|\epsilon|$  (because of large overlap number of junctions) and a cross-over of the  $p > p_c$  branch to saturation due to finite size at  $|\epsilon| \rightarrow 0$ , which is the reason why only the steepest decay can become linear on a log-log plot.



more accurate than  $p_{c,\gamma}$  for our data in contrast to typical percolation studies, where  $p_{c,\gamma}$  is considered as the best estimate<sup>83</sup>. Accordingly, we expect also a somewhat larger error for  $p_{c,\gamma}$  of  $\gtrsim 10^{-3}$  as compared to  $p_{c,\mu}$  in contrast to the four digits accuracy to parallelize the steepest decays of both branches of  $N_w$ .

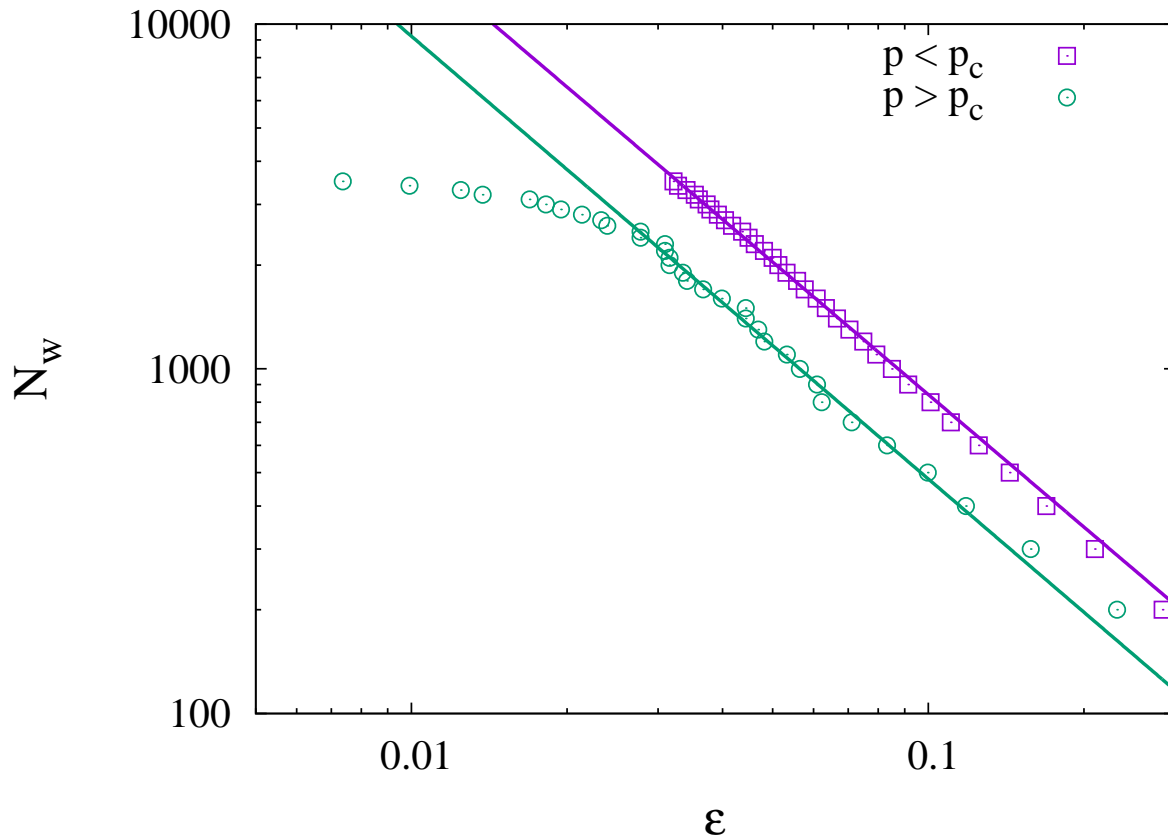


Figure 3: Plot of  $N_w$  data as a function of  $\epsilon$  for a determination of  $p_{c,\gamma}$  and  $\gamma$ . The extrapolation of the samples  $f = 6$ ,  $N = 64$  with the smallest number of cross-links and largest deviation to the predicted  $\gamma$  is shown.

The average difference between both gel point estimates is  $p_{c,\mu} - p_{c,\gamma} = 0.0012 \pm 0.004$  and thus, below the cumulated error of both estimates, which confirms the consistency of our analysis. Note that this difference is about one order of magnitude smaller than the observed smallest gap between  $p_{c,\text{id}} + \Delta p$  and our estimates  $p_{c,\mu}$  or  $p_{c,\gamma}$ . Therefore, the observation of this gap is significant and we present below an analysis of the scaling of the gel point based upon  $p_{c,\mu}$  that we consider as our best estimate. Nevertheless, an additional test using  $p_{c,\gamma}$

is included in Figure 6 and 7, which confirms in each case the observed scaling of  $p_{c,\mu}$  within error bars.

For our finite simulations, a  $\gamma$  between mean field and critical percolation is found, with the tendency that smaller samples and samples with a higher overlap number are closer to the mean field prediction. This is a typical observation for finite samples within medium-range bond percolation problem<sup>42</sup>, since the number of independent volumes in one direction scales as  $L/R$ , where  $L$  is the lattice size and  $R$  the range of the bonds. For  $L/R = 1$ , one reaches the mean field limit as bonds can be introduced between any pair of nodes, while for  $R \approx bN^{1/3}/\phi$ , one arrives at the classical bond percolation limit. Our simulation data spans only a rather small range of  $L/R$  and the error for  $\gamma$  is rather large such that a detailed analysis of the cross-over scaling is not much meaningful.

The ratio of the coefficients of the two power law fits below and above the gel point,  $C_-/C_+$ , is also provided in Table 1. For this ratio, a value of  $\approx 10$  is expected for percolation in three dimensions while kinetic gelation provides  $C_-/C_+ \approx 3$  with the possibility that  $C_-/C_+ \rightarrow 1$  in the limit of mean field (diverging overlap number)<sup>44</sup>. A similar tendency is found for the ratio  $C_-/C_+$  that tends towards unity when  $\gamma$  approaches one while it is largest for the samples with largest  $\gamma$ . However, a more detailed analysis of  $C_-/C_+$  as for the cross-over scaling of the exponents is not possible within the limited data of the present study and subject of ongoing research.

## Scaling of the gel point shift

The first goal of the present paper is to demonstrate that the true gel point does not overlap with estimates based upon intra-molecular reactions. Therefore, we take  $p_{c,\mu}$  as our best estimate for the true gel point and compare with the upper bound for a mean field estimate with a correction for cyclization,  $p_{c,\text{id}} + \Delta p$  in Figure 4. The data are plotted as a function of  $N$  in order to check whether the shift of the gel point scales with the overlap number of

elastic strands in melt as proposed in mean field models. This is observed indeed for the  $\Delta p$  data but not for the true gel point shift  $p_{c,\mu} - p_{c,\text{id}}$ . According to the above discussion and section “intra-molecular reactions” of the Appendix, it is expected that the amount of intra-molecular reactions is independent of  $f$  in a very good approximation, which is demonstrated by the excellent collapse of the data for the self-consistent determination of  $\Delta p$  in Figure 4. This is in line with older models for the gel point shift, for instance Refs.<sup>16,17,20</sup> but disagrees with more subsequent work, for instance Refs.<sup>22,87</sup>.

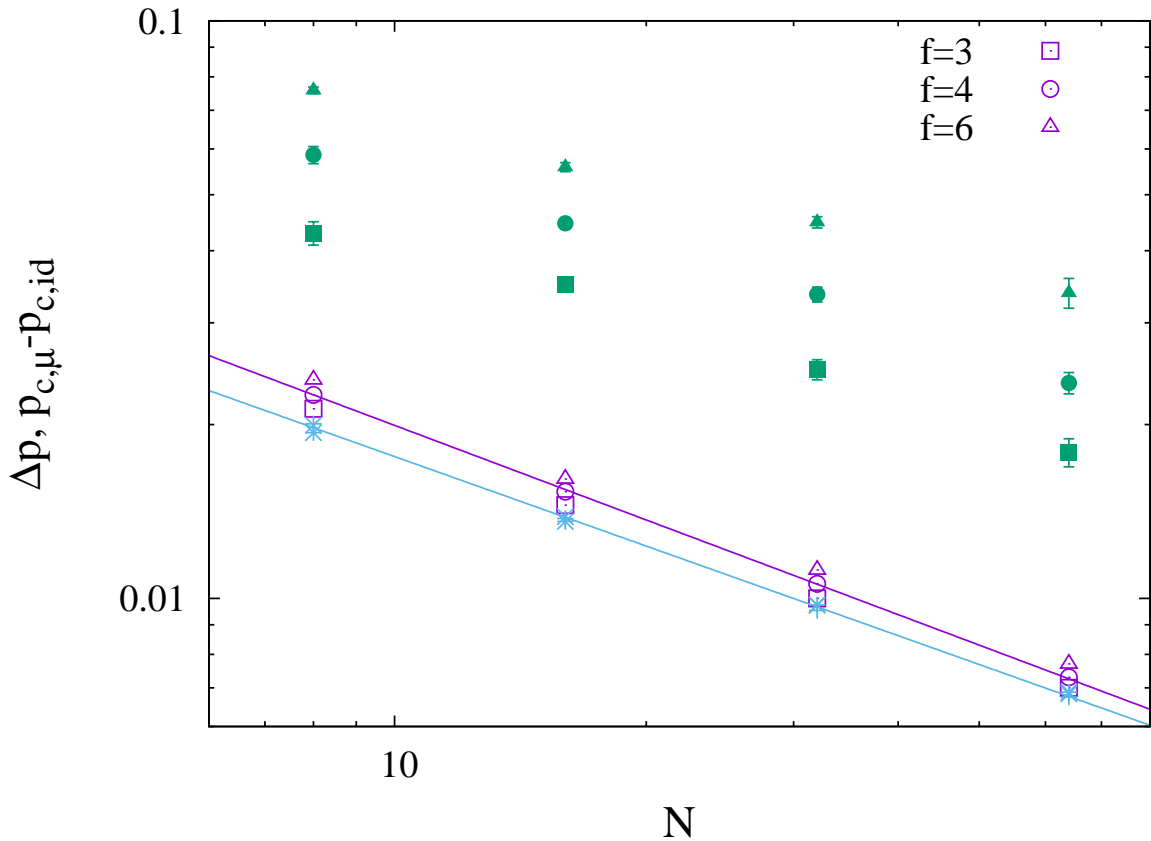


Figure 4: Gel point shift as obtained from modulus,  $p_{c,\mu} - p_{c,\text{id}}$  (full symbols) compared with  $\Delta p$  as measured at the peak of  $N_w$  (open symbols) or in self-consistent manner (plus, times, and star symbols for  $f = 3, 4,$  and  $6$  respectively) at a conversion of  $p_{c,\text{id}} + \Delta p$ . The upper line is a power law decay for  $\Delta p = cN^{-\alpha}$  with  $c = 0.070 \pm 0.004$  and  $\alpha = 0.54 \pm 0.03$ , the lower line a similar power law decay with  $c = 0.057 \pm 0.001$  and  $\alpha = 0.52 \pm 0.01$ .

The second interesting observation of Figure 4 is that  $p_{c,\mu} - p_{c,\text{id}}$  is neither in quantitative nor in qualitative agreement with  $\Delta p$  and is indeed an explicit function of  $f$  (similar results

are found for  $p_{c,\gamma} - p_{c,\text{id}}$ ). In a recent paper on a two-dimensional long range percolation problem, it was shown that the shift of the gel point with respect to mean field (for small deviations from mean field) is a power law function of the number of accessible neighbors<sup>42</sup>. We expect a similar behavior in three dimensions based upon the overlap number of sites (cross-links)  $P$ . Indeed, a collapse of the  $p_{c,\mu} - p_{c,\text{id}}$  data are obtained for a scaling variable  $P \propto N^{1/2}/f$  for our cross-linked melts, see Figure 5.

An overlap of the data as a function of the overlap number of chains  $\propto N^{1/2}$  has been emphasized previously<sup>22</sup> and was proposed in other models on the gel point shift<sup>16-18,88</sup> due to the expected dependence of  $\Delta p$  on  $N^{1/2}$  as discussed above. However in Ref.<sup>22</sup>, only data with  $f = 4$  were analyzed. Therefore we compare in section “Experimental gel point data” of the Appendix the gel point data of several studies for networks made of similar chemistry but different  $f$ . Unfortunately, the available experimental data are not fully conclusive, since not all data show exactly the same trend. Nevertheless, the common result is that any set of data exhibits clear power law dependence  $P^{-\alpha}$  for the observed delay of the gel point. The data for the PDMS systems in<sup>88</sup> is in excellent agreement with the proposed dependence on  $f$ , while there is only fair agreement in this respect for the PU systems as discussed in the Appendix. Cail and Stepto<sup>88</sup> point out that the mean field prediction for the amount of loops underestimates the real shift of the gel point by a factor of four to seven (a factor of two to five for our simulation data). Therefore, neither for these experimental data nor for our simulations, there is a quantitative match of the gel point shift with the amount of intra-molecular reactions at the gel point.

In general, there is  $P \propto \phi N^{1/2}/f \propto (V_{\text{dry}}/V)$  for networks prepared in semi-dilute solutions with theta solvents and  $P \propto (V_{\text{dry}}/V)^{0.65}$  in good solvents using standard scaling relations for  $R$  in both cases<sup>8</sup>. Here, we used  $V_{\text{dry}}$  for the “dry” volume of the polymers and  $V$  for the volume of the solution at preparation conditions. Note that the scaling  $\propto N^{1/2}$  is only asymptotically correct, since corrections to polymer size due to an incompletely screened excluded volume<sup>89</sup> are neglected above. Furthermore, we have to restrict our discussion to

the case of  $P > 1$  in order to avoid a significant impact of diffusion as discussed in the introduction. A fit of the data shows that the shift of the gel point scales as  $P^{-\alpha}$  with a power  $\alpha \approx 0.78 \pm 0.03$ . Note that data at the same  $P/f$  but different  $f$  refers to samples containing a different number of junctions, since all samples were simulated in a box of size  $L = 256$  lattice units. Since these data superimpose for our scaling variable, we do not expect a dramatic effect of finite size corrections for our gel point estimates.

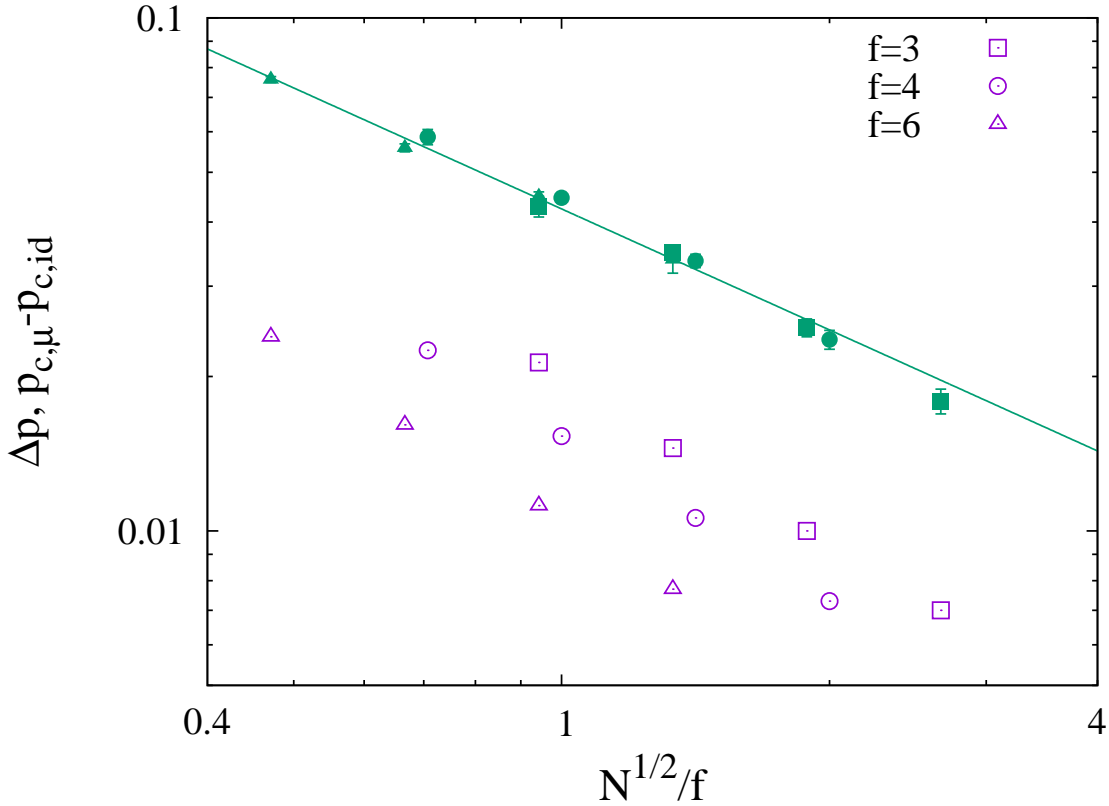


Figure 5: Gel point shift as obtained from extrapolation of modulus data,  $p_{c,\mu} - p_{c,id}$  (full symbols) compared with  $\Delta p$  as measured at the peak of  $N_w$  (open symbols). The line is a power law decay  $c (N^{1/2}/f)^{-\alpha}$  with  $c = 0.0424 \pm 0.0005$  and  $\alpha = 0.78 \pm 0.03$ .

The above analysis is equivalent to raw experimental data where no corrections to scaling have been considered. Figure 6 contains a more accurate analysis that corrects for unequal reactivity and composition fluctuations by relating the true gel point to  $p_d$  instead of  $p_{c,id}$ . On experimental side, a similar analysis could be conducted using network disassembly

spectrometry (NDS)<sup>90</sup> next to the critical point. As a result, we obtain a slightly smaller  $\alpha$  close to  $2/3$ . Recall that  $p_d < p_{c,id}$  for our samples, since the corrections are dominated by composition fluctuations. Therefore, a larger  $\alpha$  from experimental data on end-linking of model networks as compared to an apparent  $\alpha \approx 2/3$  can be taken as a possible indication of imperfect mixing. Indeed, this discussion is supported by experimental studies, see section “Experimental gel point data” of the Appendix for more details. In brief, the exponents  $\alpha$  that one obtains from the data of Refs.<sup>88,91–94</sup> as a function of the chain overlap number ranges from 0.63 up to 1.36. In several cases where large exponents  $\alpha > 1$  are fit to the experimental data, the authors of the original works mention systematic deviations from other studies and suspect unequal reactivity or mixing problems to be the reason for these changes.

So far, we have only considered the total delay of the gel point. Clearly, if one introduces a new bond into the system, this bond either connects two nodes of the same cluster or two nodes of different clusters. Thus, the contributions of intra-molecular reactions and XB to the gel point delay are disjoint and we can single out the XB contribution by analyzing  $p_c - (p_d + \Delta p)$ . In this respect, we have to mention that intra-molecular reactions are by far more important for GS as compared to percolation when comparing data for systems with the same number of neighbors. The reason for this difference is that loops with  $i \leq 2$  can be formed in GS, which are typically forbidden in bond percolation models. Since the size distribution of loops decays quickly as  $i^{-5/2}$ , this yields almost one order of magnitude more intra-molecular reactions for GS as compared to percolation problems with a similar number of accessible neighbors. Thus, if XB is the main source for a shift of the critical point away from the mean field gel point in percolation problems, one must not necessarily expect the same for polymer gelation.

Above, we have not accounted for long range bond correlations that lead to an apparent swelling of chain size<sup>60,89,95</sup>. This can be corrected by including more accurate estimates for the size of the chain end-to-end vector  $R$  in equation (1), see for instance, equation

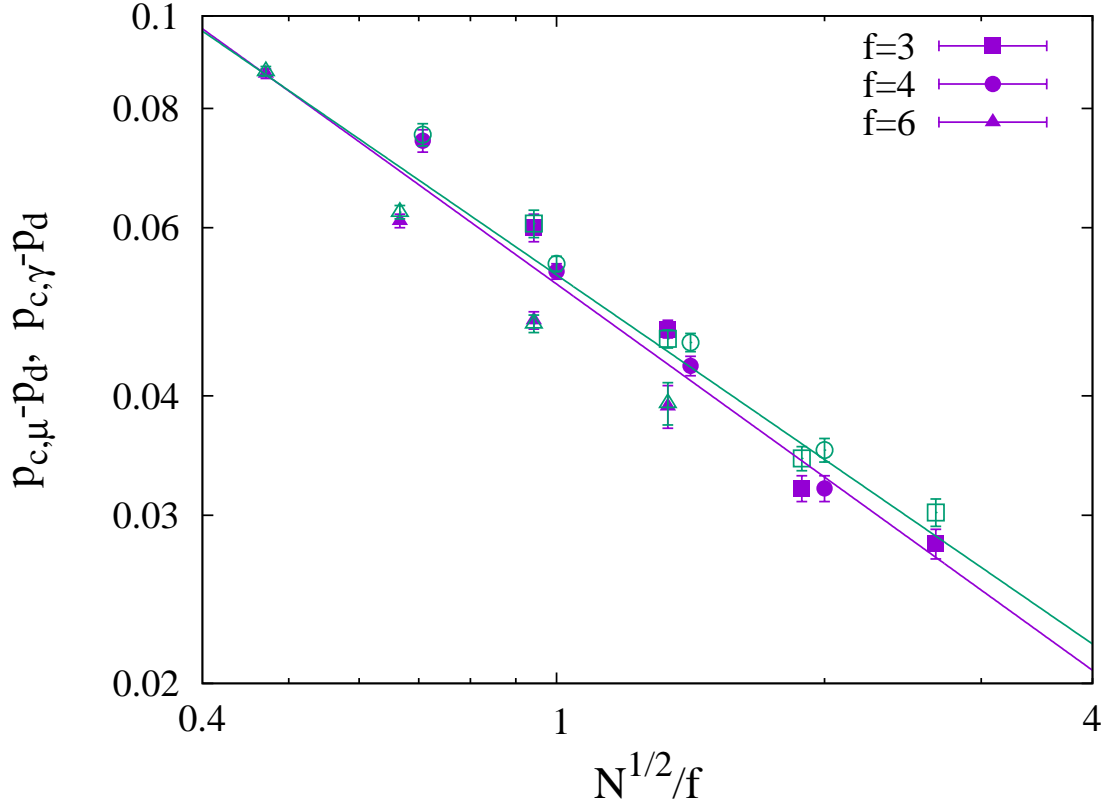


Figure 6: Gel point shift as obtained from modulus data,  $p_{c,\mu} - p_d$  (full symbols) compared with gel point shift from peak of  $N_w$  data,  $p_{c,\gamma} - p_d$  (open symbols). The lines are power law decays  $c(N^{1/2}/f)^{-\alpha}$  with  $c = 0.052 \pm 0.001$  and  $\alpha = 0.67 \pm 0.06$  (for modulus data) and  $c = 0.054 \pm 0.001$  and  $\alpha = 0.64 \pm 0.06$  for the  $N_w$  data.

(7) of Ref.<sup>89</sup> with the corresponding corrections for our simulation model. In effect, the consideration of non-ideal chain conformations stretches and shifts the data along the  $x$ -axis, which causes a smaller exponent  $\alpha$ . A qualitatively similar correction is obtained when subtracting  $\Delta p$ , since  $\Delta p$  decays quicker than  $p_c - p_d$ , see Figure 4. If both corrections are applied, the exponent is reduced from  $\alpha \approx 2/3$  to  $\alpha \approx 0.56$ . Further reduction of the exponent results from plotting the data as a function of the number of accessible neighbors,  $P-1$ , in order to introduce the same abscissa as in percolation studies ( $P-1$  is the equivalent of the coordination number of the lattice). These modifications lead in total to  $\alpha \approx 0.47$  (based upon modulus data), see Figure 7. Note that similar corrections can be included when analyzing experimental data, since the size of the molecules can be measured and  $\Delta p$  is also accessible through NDS<sup>90</sup>.

Figure 7 still does not indicate a large systematic shift of the  $p_c - (p_d + \Delta p)$  data for samples with a different number of nodes (data at same  $P$  but for different  $f$ ). This supports our proposal that finite size corrections will not lead to a dramatic modification of  $\alpha$ . A more detailed finite size analysis with an exact determination of the exponent  $\alpha$  requires samples of a range of different sizes. For this purpose, we currently develop a specialized simulation approach for our particular bond percolation problem as part of ongoing work. Quantitatively, we expect a weak increase of  $\alpha$ , since finite size effects lead to an underestimation of  $p_c$ , whereby this underestimation is larger for samples with a smaller ratio  $L/R$  (i. e. larger  $N$  and larger  $P$ ). Thus,  $\alpha \approx 0.47$  should be considered as a lower bound for the true exponent  $\alpha$  of macroscopic samples.

Below, we develop a rough idea where one could expect the exponent  $\alpha$  from theoretical side by comparison with recent work on “long range” percolation, Ref.<sup>42</sup>. In this work,  $z \sim R^d$  is the number of accessible neighbors in the percolation problem, where  $R$  is the range up to which bonds can be formed and  $d$  is the space dimension. Our quantity of interest,  $p_c - (p_d + \Delta p)$ , is approximately  $zp_c - 1$  in Ref.<sup>42</sup> and we follow the discussion around Figure 13 in Ref.<sup>42</sup>. Note that conversion  $p$  (and thus,  $p_c$ ) is normalized in Ref.<sup>42</sup> to the maximum



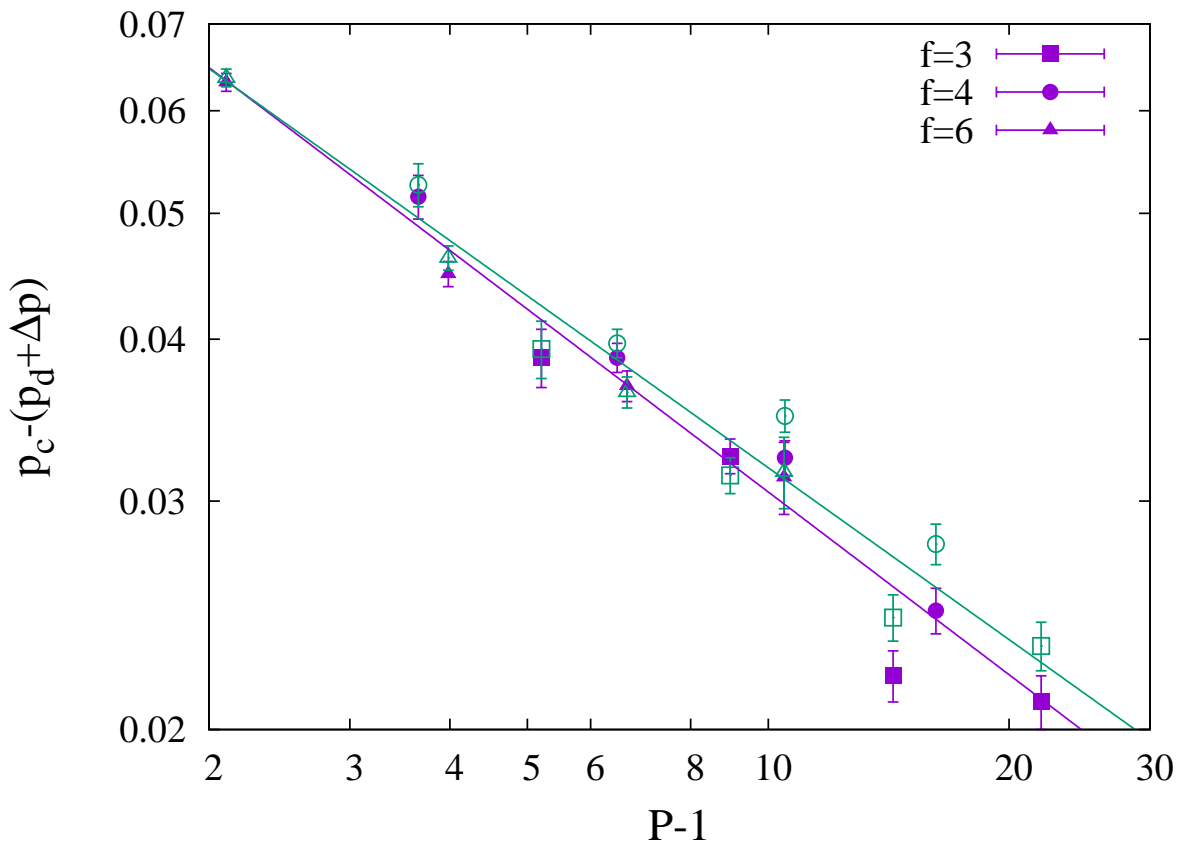


Figure 7: XB contribution to the gel point shift as obtained from either modulus data (full symbols) or  $N_w$  data (open symbols) with corrections for chain size and unequal reactivity. The lines are power law decays  $c(P - 1)^{-\alpha}$  with  $c = 0.090 \pm 0.004$  and  $\alpha = 0.47 \pm 0.03$  (for modulus data) and  $c = 0.088 \pm 0.004$  and  $\alpha = 0.44 \pm 0.03$  for the  $N_w$  data.

possible number of bonds per node, which is  $z$ . In contrast to this, the maximum number of bonds is  $f$  in GS and depends neither on  $R$  nor  $d$ . The second, more subtle difference between GS and long range percolation is that the bonds (the polymer molecules) fill space for GS, while the nodes fill space for the percolation problem. Thus, there is  $P \propto 1/f$  and both, the range  $R$  and the overlap number scale with  $N^{1/2}$  in GS. Thus,  $P \propto R$  for GS while  $z \sim R^d$  in percolation problems.

In order to derive an estimate for  $\alpha$ , let us assume that for sufficiently large  $f$ , the differences between a finite fixed  $f$  and a node valence that grows  $\propto z$  are not largely relevant at  $p_c$ , since  $zp_c \approx 1$  next to the mean field critical point. Furthermore,  $P \propto 1/f$  rescales density for GS by a constant factor and thus, the number of neighbors  $P - 1$  that corresponds to  $z$  is the key variable for scaling. Then, let us parametrize the neighborhood of the MF fixed point (the limit of  $R \rightarrow \infty$ ) with a temperature variable  $v_t$  and a range parameter  $v_r$  such that these variables rescale as  $v_t(s) = s^{y_t^*} v_t$  and  $v_r(s) = s^{y_r^*} v_r$  under a scale factor  $s$ . The exponents  $y_t^*$  and  $y_r^*$  are the effective mean field renormalization exponents next to the mean field fixed point<sup>42</sup>.  $y_t^* = 1$  for  $d = 3$  renormalizes the “temperature scale” (this exponent is equivalent to  $1/\nu$  where  $\nu$  is the exponent that describes the divergence of the correlation length in percolation problems)<sup>42</sup> and  $y_r^* = 2/3$  (for  $d = 3$ )<sup>96</sup> renormalizes an inverse interaction range. Note that we have kept the notation of Ref.<sup>42</sup> for a better comparison with previous work and readers should not get confused by an index  $t$  (temperature plays no role for percolation). In fact, the discussion in Ref.<sup>42</sup> makes use of general results for the  $q$ -state Potts model that were obtained within the Ising class ( $q = 2$ ) where temperature is the key variable, but apply also for the percolation problem ( $q = 1$ ), see Ref.<sup>42</sup> for more details. For classical long range percolation problems, there is  $R^{-1} \sim z^{-1/d}$  in the mean field limit with  $z \rightarrow \infty$ . Therefore,

$$v_t(s) \propto v_r(s)^{y_t^*/y_r^*} \propto R^{-3/2} \propto z^{-1/2} \quad (11)$$

in 3 dimensions. By analogy, we approximate  $p_c - (p_d + \Delta p) \approx v_t$  (ingoring small finite loop contributions). We further identify  $z = P - 1$ . Given that this analogy and identification are correct, we obtain

$$p_c - (p_d + \Delta p) \propto (P - 1)^{-\alpha} \quad (12)$$

with  $\alpha = 1/2$  as the exponent for the XB contribution (finite  $z$  correction beyond finite loops) to the delay of the gel point in macroscopic samples.

Our lower bound estimate  $\alpha \approx 0.47$  agrees well with this rough estimate even though  $f$  and  $P$  are far from the asymptotic limit. Also, the difference between both estimates is sufficiently small to agree with the proposal of a weak impact of finite size on  $\alpha$  that we made above. However, there is still the possibility that finite  $f$  corrections compensate significant finite size corrections, which we cannot disentangle based upon our limited set of data. Additional simulations on the percolation problem that is equivalent to GS will help to clarify the above proposal of  $\alpha = 1/2$  and are part of ongoing work.

One interesting aspect of our discussion is that the width of the Ginzburg zone grows quicker towards smaller  $P$  as compared to the gel point delay,  $\epsilon_G / [p_c - (p_d + \Delta p)] \approx P^{-1/6}$ . Such a qualitative trend allows to accommodate the requirement of extra bonds due to both XB and loop formation within the Ginzburg zone for a significant range of  $P > 1$  (several orders of magnitude in  $P$ ), since the coefficient for  $\epsilon_G$  is of order unity<sup>97</sup>, while the coefficient of XB is  $c \approx 0.09$ . Therefore, we expect that  $\alpha \approx 1/2$  may apply for virtually all experimental data. Loop formation may dominate over XB corrections only in the limit of  $P < 1$ , see Figure 7, where the percolation model breaks down anyways. Conversely, we infer that the width of the Ginzburg zone provides a natural upper bound for  $\alpha$ , thus,  $\alpha \leq 2/3$ . Since the gel point must be located within the Ginzburg zone, a cross-over of  $\alpha$  to this upper bound may be enforced at very large  $P$ . Altogether, our estimate for  $\alpha$ , the simulation results at the available limited  $P$ , and the known scaling of the Ginzburg zone are not in conflict for the parameter range of interest,  $P > 1$ .

# Summary

We have demonstrated that the position of the gel point cannot be estimated by considering intra-molecular reactions as the only correction to mean field, even though cyclization is well approximated by mean field. Instead, the largest contribution to the gel point delay is due to the extra bonds (XB) required to build the connections between the non-overlapping giant molecules. Our data and discussion indicate that this XB contribution decays roughly as  $(P - 1)^{-1/2}$  in contrast to the contribution of finite loops, which decays approximately as  $N^{-1/2} \propto f/P$  for large junction overlap number  $P$ . Beyond these two main contributions, there are corrections due to composition fluctuations and unequal reactivity, non-ideal chain size, and due to the transition from junction overlap number  $P$  to number of neighbors  $P - 1$ . Finite size corrections are likely to contribute only little to scaling, since we observe no large shift of the different data at same  $P$  but different  $f$ . Some of the corrections (unequal reactivity and composition fluctuations) could be avoided by analyzing the homo-polymerization of  $f$ -arm star molecules as model systems. Other corrections like non-ideal chain conformations and contribution of small cycles are accessible through additional measurements, which allows to repeat our analysis with experimental data.

# Acknowledgement

We thank the ZIH Dresden for a generous grant of computation time and the DFG for funding Project LA2735/5-1. We further thank Y. Deng for stimulating discussions on medium range percolation.

# Appendix

## Intra-molecular reactions

Loops (cyclic structures in the reaction bath) are analyzed using a spanning tree approach<sup>61</sup> to assure that no loop is counted twice and that their total number equals the cycle rank  $\xi$ . It has been shown by computer simulations<sup>36</sup> that the frequency  $L_i$  of finite loops made of  $i$  precursor polymers scales at the gel point approximately as predicted by mean field<sup>20,62</sup>

$$L_i(p_c) \propto i^{-5/2}. \quad (13)$$

Note that within the mean field approximation, the expected average number of junctions in generation  $i$  apart from a given junction is exactly unity at the gel point independent of junction functionality  $f$ . Thus, also the total amount of loops next to the gel point is independent of  $f$  in a good approximation, see Figure 4. Note that integration over the ideal reaction rate, equation (20) of Ref.<sup>36</sup>, up to the gel point, turns the  $i^{-d/2}$  dependence for the return probability of a random walk in  $d$  dimensions to  $i^{-d/2-1}$  for the (mean field) loop size distribution at the gel point. In case of excessive loop formation, the above power law may not be reached for the smallest  $i$ , see also equation (A2-44) of Ref.<sup>62</sup>.

Loop formation is not excessive for our simulations and the proposed power law is reached in a good approximation between a conversion of  $p = 0.64$  and  $p = 0.65$ , see Figure 8. But according to Table 1, the data at  $p = 0.60$  of Figure 8 refers to the gel point as estimated from intra-molecular reactions,  $p_{c,\text{id}} + \Delta p$ . In contrast to this, the loop size distribution at  $p = 0.60$  is typical for  $p < p_c$ , where a cut-off for the size distribution near a finite  $i$  reflects the average number of strands between pairs of reactive groups of the characteristic molecule, see section “Mean field estimates of the gel point”. At the gel point, the degree of polymerization of the characteristic molecule diverges and thus, the position of the cut-off shifts towards infinity. In fact, a cross-over to a second weaker power law at large  $i \approx 20$  is expected near  $p_c$  which is essentially lost in the noise of the data at  $i \geq 20$ .

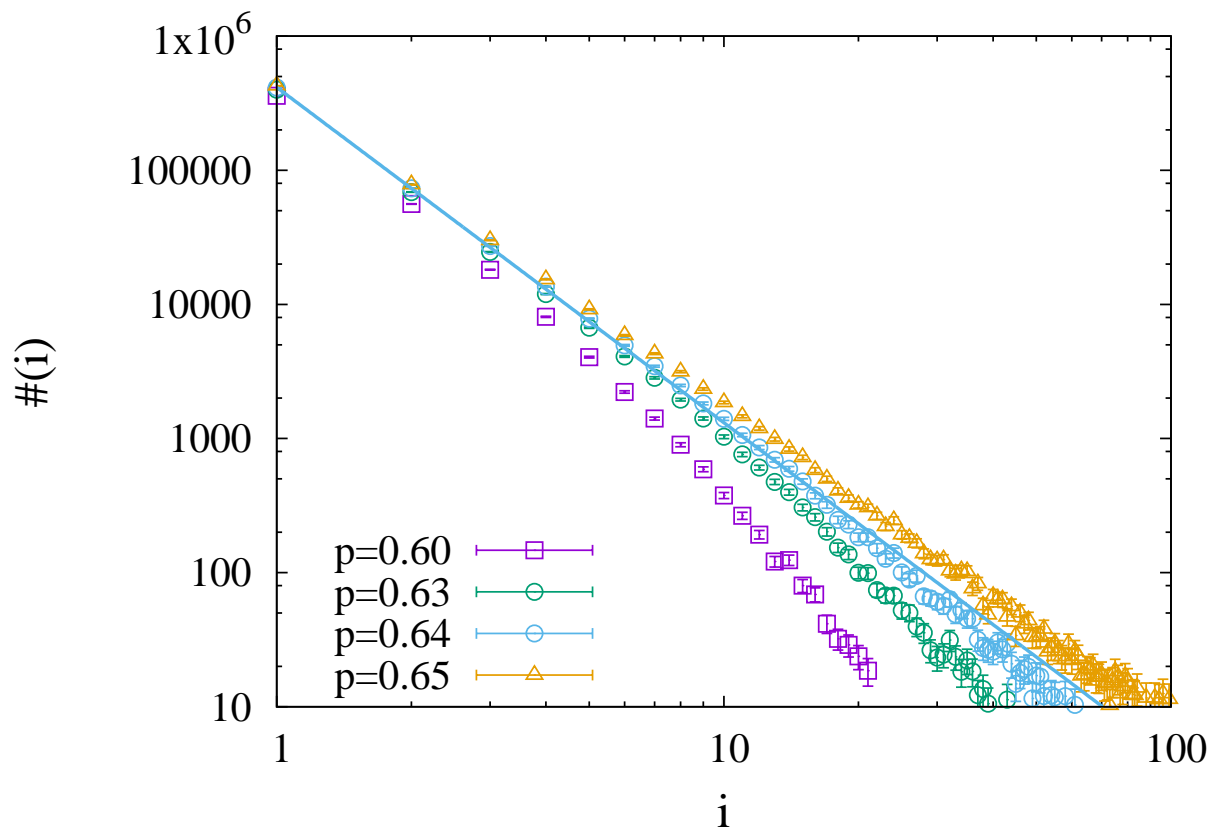


Figure 8: Total number of loops,  $\#(i)$  made of  $i$  strands in the vicinity of the gel point for the 100 networks with  $f = 4$  and  $N = 8$ . The line indicates a power law decay with exponent  $-5/2$ .

## Unequal reactivity

Let us consider systems with a stoichiometric ratio  $r = 1$  of the reactive groups on chain ends and on junctions. In the mean field model, the reactivity of all reactive groups is identical. The probability that an  $f$ -functional junction has  $j$  bonds to chain ends is then described by the binomial distribution

$$P(X_j) = \binom{f}{j} p^j (1-p)^{f-j}. \quad (14)$$

In similar manner, one can compute the connectivity distribution of chains by considering them as two functional units,  $f = 2$ .

A fully equivalent treatment to this statistical discussion is to consider reaction rates  $k_j \propto f - j$  for the rate equations

$$\frac{dc_0}{dt} = -k_0 c_0 c_e \quad (15)$$

for  $j = 0$  and

$$\frac{dc_j}{dt} = [k_{j-1} c_{j-1} - k_j c_j] c_e \quad (16)$$

for  $0 < j < f$  and

$$\frac{dc_f}{dt} = k_{f-1} c_{f-1} c_e \quad (17)$$

for  $j = f$  (and a similar scheme for chains that are two-functional). Here,  $c_j$  is the concentration of junctions with  $j$  bonds,  $c_e$  is the concentration of the reaction partners (the chain ends). By selecting reaction rates  $k_j \propto f - j$  one takes into account that there are  $f - j$  non-reacted groups per molecule with same reactivity. For stoichiometric systems, one arrives after some algebra (and considering  $dp/dt$ ) at equation 14.

In case of end-linked model networks, the network junctions are less accessible to reactions and less mobile with increasing number of chains attached. Thus, we expect that the reaction rates  $k_j$  are no more  $\propto f - j$ . Instead, there will be comparatively smaller reaction rates the

larger the  $j$ . Such a behavior leads qualitatively to a quicker decay of  $c_0$  and a delay of the increase of  $c_f$  as compared to the statistical case, when plotting the corresponding  $P(X_j)$  as a function of  $p$ . Intermediate states  $0 < j < f$  will exhibit a narrower peak as a function of  $p$ .

Copolymerizations are inevitably subject to composition fluctuations of the two species. Composition fluctuations will increase  $P(X_j)$  where  $P(X_j)$  is convex and will decrease  $P(X_j)$  within concave domains as composition fluctuations can be modeled by a spontaneous split of the system into two domains of somewhat larger and smaller conversions (similar to the discussion of the phase behavior of polymer solutions in text books where concentration fluctuations are considered). On a qualitative basis, we expect for dominating corrections due to composition fluctuations that  $P(X_0)$  and  $P(X_f)$  will be enlarged as compared to the statistical prediction, since these are convex for all  $p$ , which is the opposite trend as expected from accessibility and mobility.

Both effects discussed above are visible in the connectivity distributions of junctions and chains, see Figure 9 and Figure 10. Junctions are initially single monomers, which react clearly quicker than junctions attached to chain ends. Here, the impact of a different mobility dominates. On the other hand,  $P(X_f)$  and  $P(M_2)$  appear to be dominated by the impact of composition fluctuations. Altogether, there are significant deviations from the ideal case, equation (14). These must be taken into account for an exact mean field estimate of the critical point.

Non-ideal systems are readily mapped onto the corresponding ideal systems by considering appropriate distributions of junction and chain functionality. The experimental data for  $P(X_j)$  and  $P(M_j)$  at a given conversion  $p$  are considered to be equivalent to a model system at full conversion with a functionality distribution of junctions and chains that is identical to  $P(X_j)$  and  $P(M_j)$ . Then, equation (24) to equation (33) of Ref.<sup>13</sup> can be used to compute numerically the “effective” functionalities  $f_e$  and  $g_e$  of junctions and chains, respectively. The



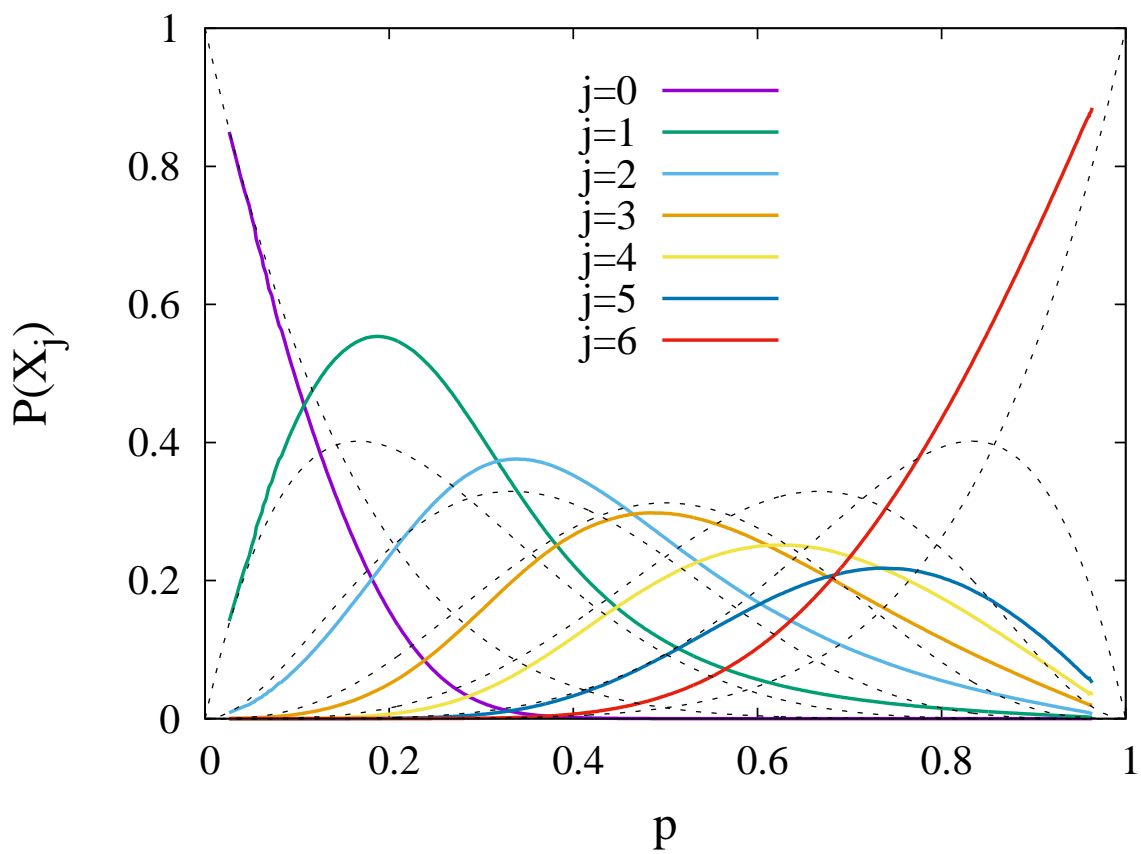


Figure 9: Distribution of the number  $j$  of connections to chain ends for junctions  $X$  with  $f = 6$  in networks with  $N = 32$ . Colored lines show simulation data, dashed black lines are the binomial distribution, equation (14).

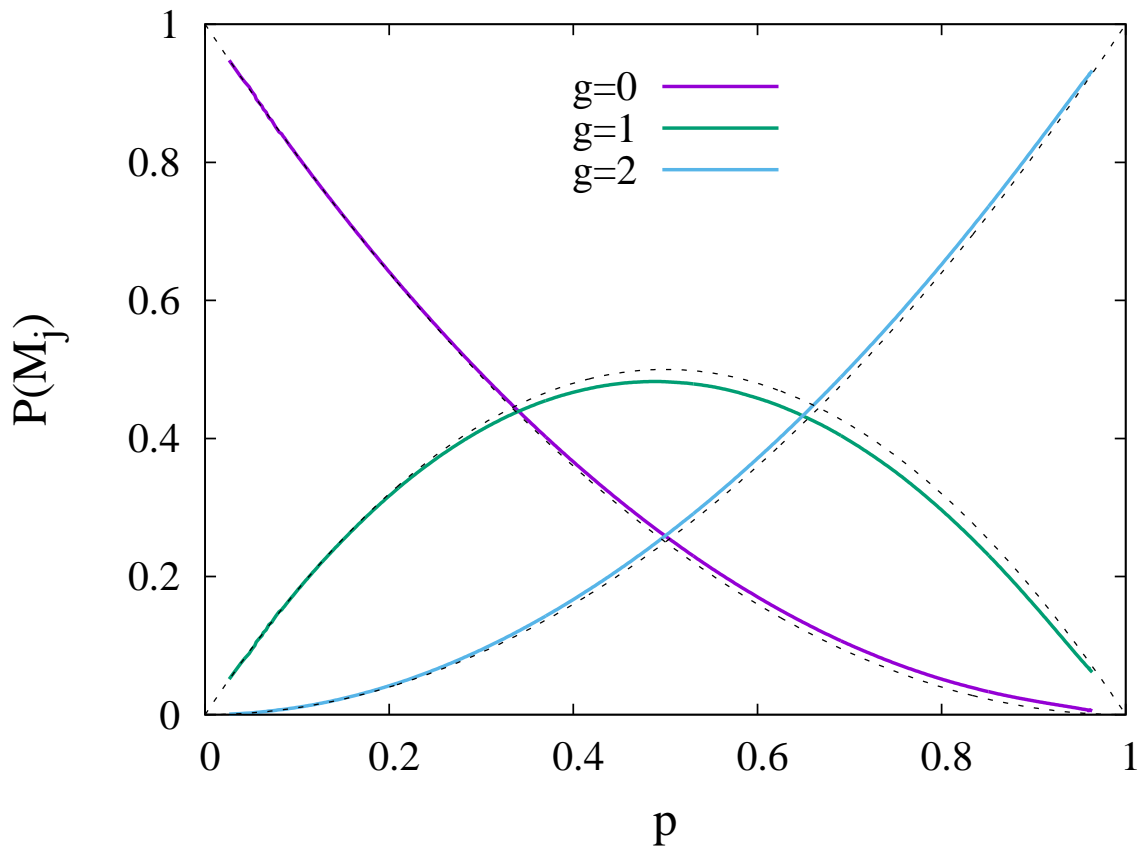


Figure 10: Distribution of the number  $j$  of connections to junctions for chains  $M$  in networks with  $f = 6$  and  $N = 32$ . Colored lines show simulation data, dashed black lines are the binomial distribution, equation (14).

gel point of the equivalent system is given by the condition

$$(f_e - 1)(g_e - 1) = 1, \tag{18}$$

since  $rp^2 = 1$  after the mapping of the data and  $r = 1$  for the stoichiometric systems of our study. The results for the resulting estimate of the gel point,  $p_d$ , based upon this analysis can be found in Table 1.

### Experimental gel point data

A large number of authors published experimental data on the gel point conversion in the past decades starting with the seminal paper by Flory on gelation<sup>11</sup>. Refs.<sup>88,91-94,98-102</sup> are just some examples from literature. Among these works, we have chosen Refs.<sup>88,91-94</sup> as basis for comparison, since the data is presented as (or readily converted into) a function of the so called “ring forming parameter”

$$\lambda_0 = \frac{P_a}{c_0} \tag{19}$$

that we introduce here only in its simplest possible form for a homo-polymerization of  $f$ -functional stars. In this case,  $c_0$  is the initial concentration of reactive groups and  $P_a$  is the concentration of a single reactive group of the star in the vicinity of a selected reactive group of the same star. Thus,  $1/\lambda_0$  is essentially the overlap number of reactive groups within the pervaded volume of the shortest strand that can form a loop. Thus, for reactions in bulk, there is  $N^{1/2}/f \propto (\lambda_0 f)^{-1}$ , which allows for a simple qualitative comparison of simulation data and experiment.

In Figure 11, we compare the data of the different PU systems of Ref.<sup>88</sup>. The full cloud of data points seems to support an exponent in the range of  $\alpha \approx 3/4$  for the scaling variable  $N^{1/2}/f$  while the individual data sets are more in line with a weaker decay as a function of  $N^{1/2}/f$ . Furthermore, the dependence on  $f$  is slightly weaker as for our simulation data. On the other hand, the data of the PDMS systems 1-4, fully overlaps as a function of  $f$ , see

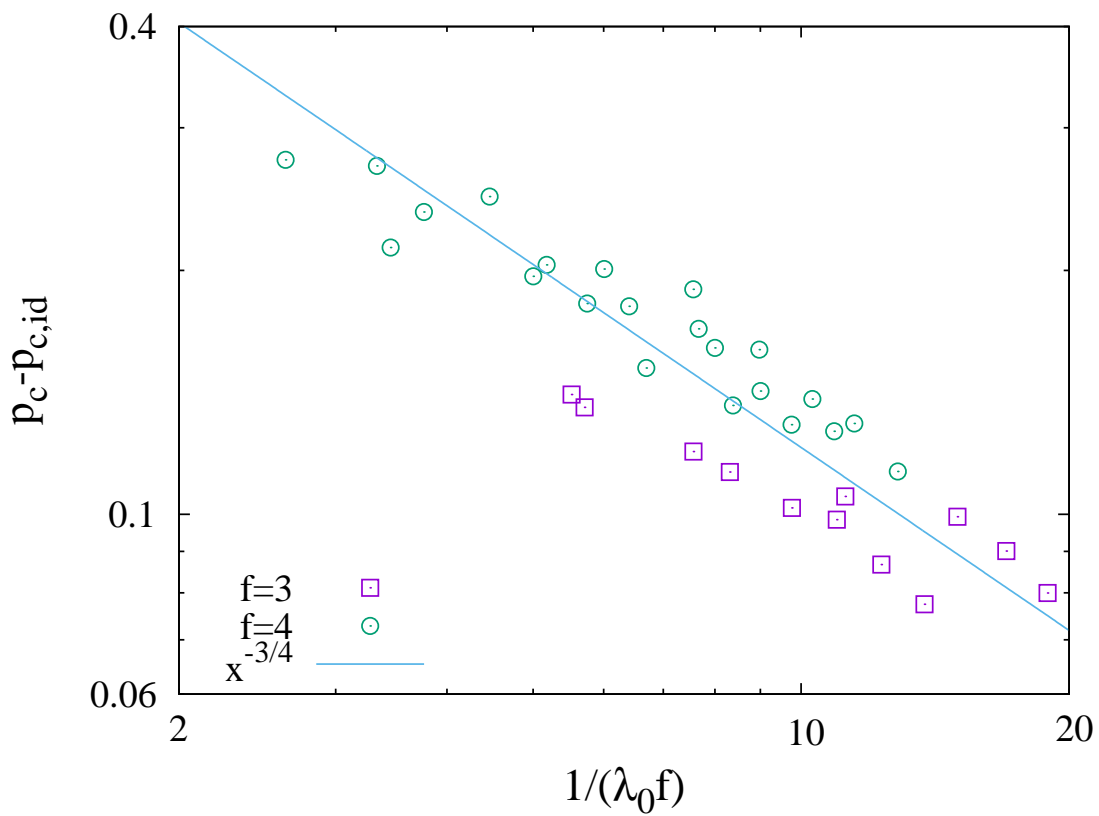


Figure 11: Collapse of the data for the poly-urethane systems PU 1-6 of Ref. <sup>88</sup> that were also discussed in Refs. <sup>86,98,103-105</sup>, where cross-linking occurred in bulk and in various dilutions in nitrobenzene. The line indicates a scaling according to  $(N^{1/2}/f)^{-3/4}$ .

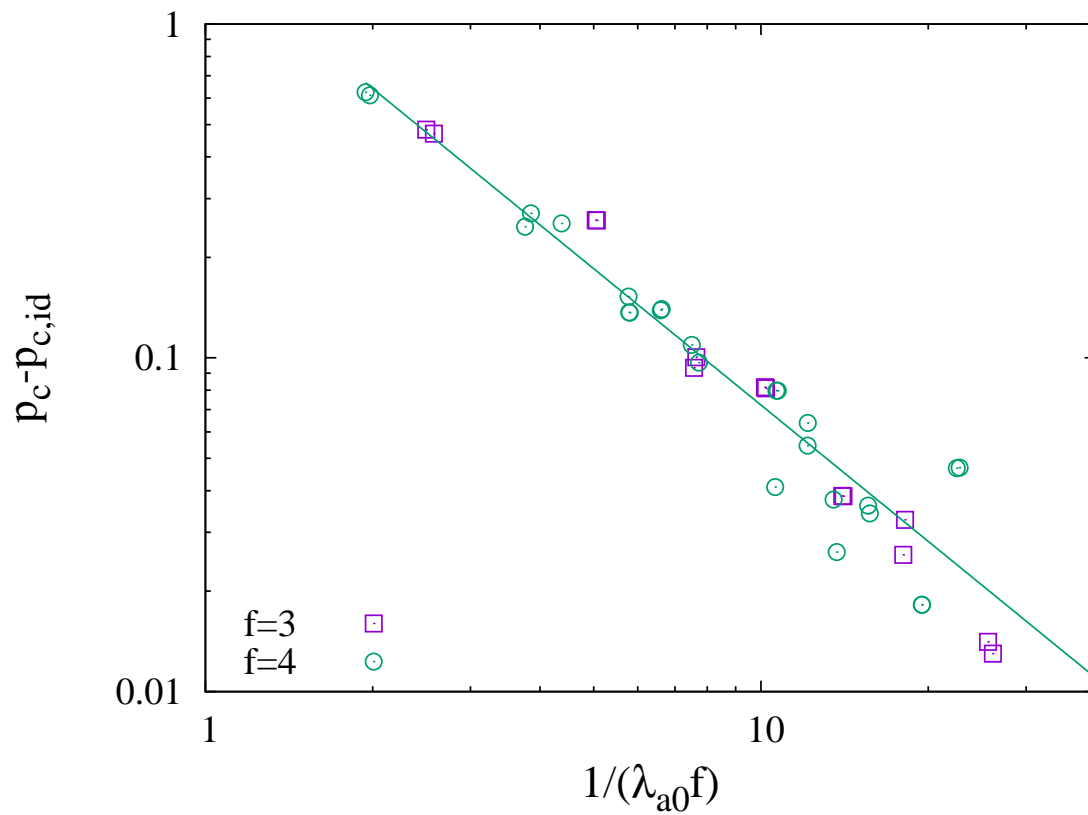


Figure 12: Collapse of the data for the poly-dimethylsiloxane systems PDMS 1-4 of Ref.<sup>88</sup> that were cross-linked in bulk or diluted by inert PDMS chains. Additional information about this data can be found in Refs.<sup>86,106</sup>.

Figure 12, but the exponent for the decay is here  $\alpha = 1.36 \pm 0.08$ , which is clearly stronger than for the PU systems or our simulation data. The authors of Ref.<sup>88</sup> were aware of these quantitative and qualitative differences and suspected mixing problems or side reactions to be responsible for the differences between the experimental data sets. Such problems were in particular pronounced for PDMS systems 5 and 6, which were not included in the plot for this very reason.

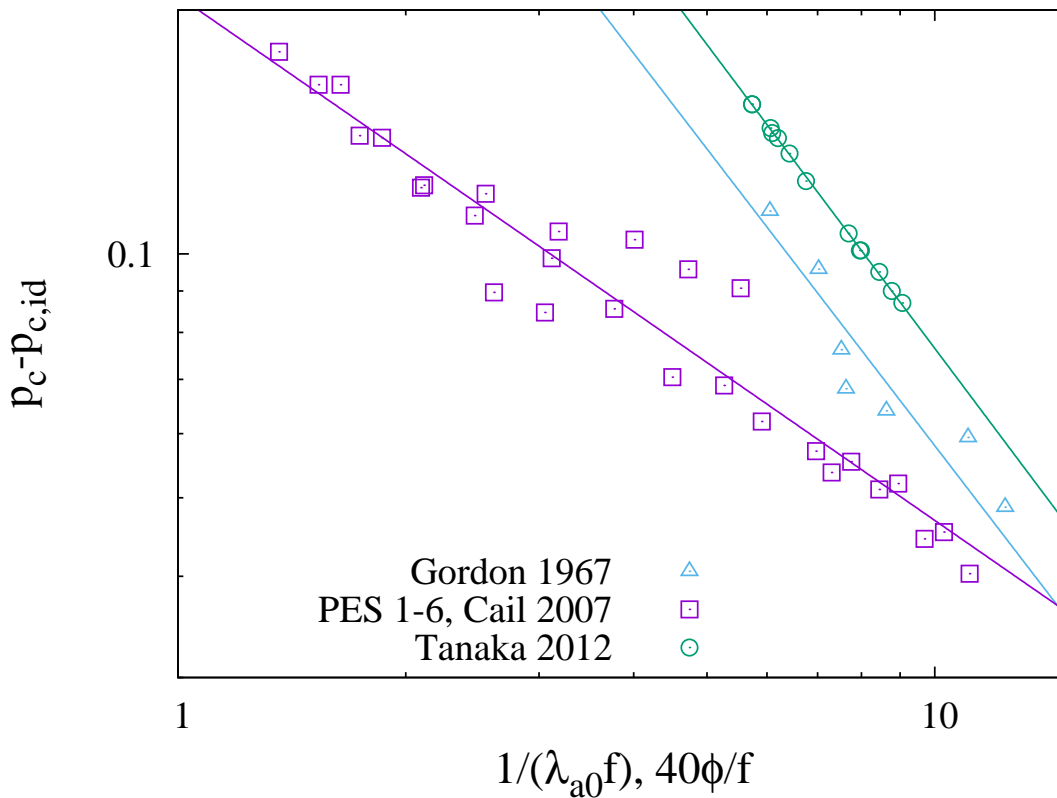


Figure 13: Gel point data of Cail and Stepto<sup>88</sup> on polyester systems PES 1-6 that were reacted in bulk or at various degrees of dilution with diglyme as solvent (additional information about this set of data is available in Refs. 1, 2 and 4 of Ref.<sup>88</sup>) and data by Tanaka *et al.*<sup>93</sup> where diglycidyl ether of bisphenol A (DGEBA) reacted with polyoxypropylene (POP) diamine of different chain lengths at various degrees of dilution with tetraglyme as solvent. Gordon and Scantlebury<sup>91</sup> provide data on reactions of adipic acid with pentaerythritol either in melt or with bis(3,6-dioxaheptyl)ether as solvent. Data was analyzed as function of  $\phi$  and shifted by an arbitrary factor of 40 to appear on the same scale as the data that was analyzed as a function of  $\lambda$ .

Cail and Stepto<sup>88</sup>, Tanaka *et al.*<sup>93</sup>, or Gordon and Scantlebury<sup>91</sup> report more gel point

data on different series of samples, see Figure 13. The observed exponents for the decay are  $\alpha = -0.65 \pm 0.04$ ,  $\alpha = -1.25 \pm 0.01$ , and  $\alpha = -1.2 \pm 0.2$  respectively, which differ significantly similar to the PDMS and PU systems discussed above. It is worthwhile to mention that unequal reactivity seems to be important for the systems reported by Tanaka et al.<sup>93</sup> where the larger exponent was recognized, which parallels in part the discussion of the PDMS systems in Ref.<sup>88</sup>. Also, Gordon and Scantlebury<sup>91</sup> argue that a substitution effect must occur to explain their set of data.

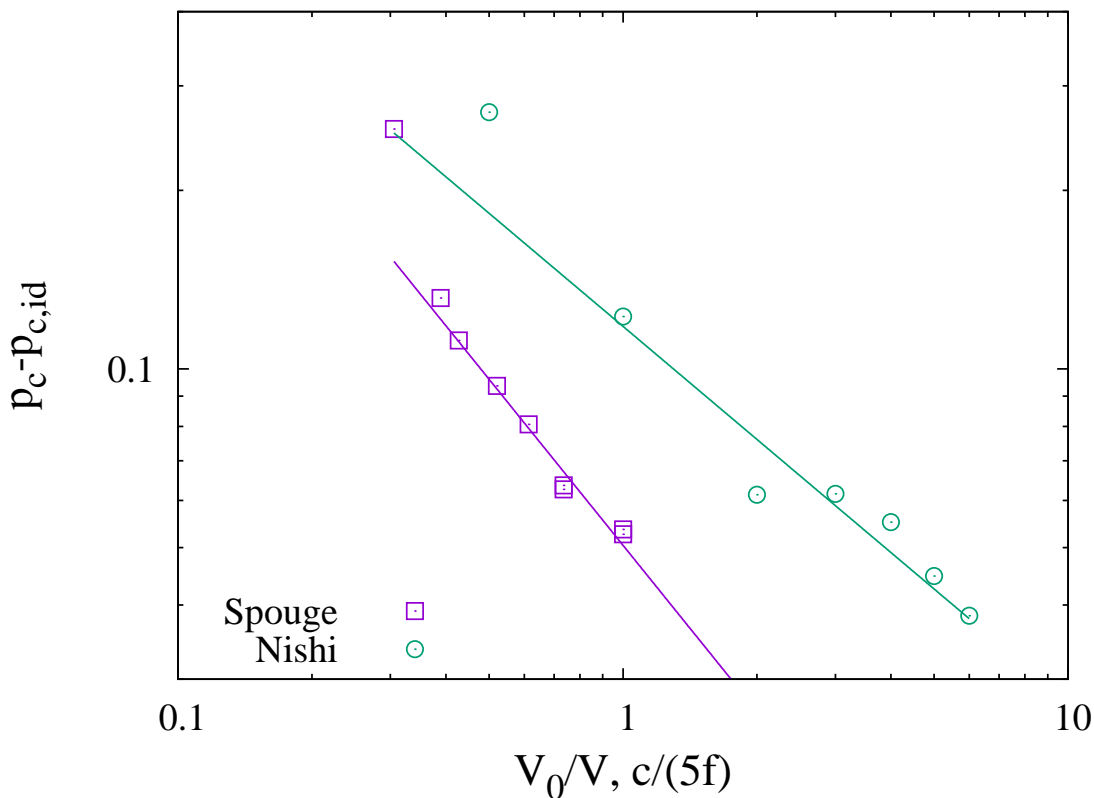


Figure 14: Gel point data of Spouge<sup>92</sup> on the reaction of adipic acid with pentaerythritol plotted as a function of  $V_0/V$  and Nishi<sup>94</sup> for the end-linking of 4-functional stars that is presented as a function of  $c/(5f)$  in gram per liter to fit on the same scale as the data of Spouge.

Spouge<sup>92</sup> discusses experimental data on the reaction of adipic acid with pentaerythritol taken from the thesis of Wile<sup>107</sup>. When plotting this data as a function of  $V_0/V$ , an exponent of  $-0.93 \pm 0.05$  is found when excluding the data at the largest degree of dilution (close

to critical dilution), see Figure 14. Recently, Nishi et al.<sup>94</sup> report gel point conversions of a copolymerization of 4-functional stars in the inset of their Figure 3, which we have plotted also in Figure 14. This particular type of reaction suppresses loops made of an odd number of elastic strands<sup>46</sup>, and thus, there are no pending loops present in these networks. Nevertheless, there is still a significant delay of the gel point with respect to the ideal gel point at  $1/(f-1)$ . The data of Nishi fits to a power of  $-0.63 \pm 0.08$  when excluding the data point at the lowest concentration (close to critical dilution) from the fit. An effect of unequal reactivity can be ignored for the end-linking of stars where all ends of the arms have the same chemistry and react only once. These exponents are in the range of our simulation data with  $\alpha \approx 2/3$  when using  $p_d$  to correct for unequal reactivity and not far from the PU and the PES systems of Ref.<sup>88</sup> with observed exponents for these systems of  $\alpha = -0.65 \pm 0.04$  and  $\alpha \approx -3/4$  respectively. Altogether, the PU and the PES systems of Ref.<sup>88</sup>, the data by Nishi et al.<sup>94</sup>, and the data of Spouge<sup>92</sup> seem to be less affected by unequal reactivity and show similar trends as our simulation data.

## Numerical Studies in Literature

The available studies can be split into two major categories depending on whether a) a mean field model is in the core of the analysis and the coordinates of all molecules are disregarded or b) the positions of the molecules in space are taken into account. Our list of examples from literature below is certainly not exhaustive and focuses on polymer specific work. Nevertheless, it should allow for a first idea about the state of the art.

Gordon and Scantlebury<sup>91</sup> use a vector of probability generating functions where loop formation is built in through a set of differential equations in the coefficients of the vector. The numerical solutions of their model are used to interpret their experimental data. This work was criticized later<sup>19</sup>, since it does not allow to fit gel point and molecular weight data with the same adjustable parameters.

The kinetic simulation method developed by Somvarsky and Dusek<sup>108</sup> is mean field en-



riched with Monte-Carlo with an explicit description of cyclization. This allows to obtain higher order molecular weights like  $N_w$ . The data of an early publication were quite noisy<sup>109</sup> while a later work<sup>110</sup> contains gel point data that were obtained under a bit artificial model for intra-molecular reactions and steric hindrance. These results are insightful on a qualitative basis, however, a quantitative analysis remains difficult as there is no obvious choice for all exponents.

Only smallest loops were considered in Ref.<sup>111</sup>. Rankin et al.<sup>112</sup> compute numerically the gel point shift from a mean field approach where only three membered rings are allowed. In both cases, the comparability with real systems that exhibit a broad distribution of loop sizes is limited.

Pereda et al.<sup>113</sup> use rate equations and a large set of different structures to model the effect of cyclization and unequal reaction rates on gelation. The numerical results show that the combination of both effects may either reinforce or partially compensate each other (depending on the choice of the parameters) even though both alone lead to a delay of the gel point.

The most recent work of the mean field class by Wang et al.<sup>22</sup> claims a quantitative prediction of gel points based upon Monte-Carlo simulation where loop formation is introduced randomly into the growing branched molecules by considering relative contact probabilities inside reactive groups along the molecular structure with a homogeneous (mean field) background of contacts with other molecules. It was found that the frequency of loops decays roughly as a power law  $i^{-5/2}$  in the vicinity of the gel point, where  $i$  is the number of linear strands per loop. The observed power changes from 2.44 to 2.73 with increasing amount of pending loops and thus, seems to be non-universal, however, such a qualitative change is expected for small  $i$  in case of excessive loop formation as mentioned in the section “intra-molecular reactions” above. The delay of the gel point was shown to be a function of the overlap number of elastic strands<sup>22</sup> and a theoretical result was obtained where  $p_c$  is given as an explicit function of junction functionality  $f$ . However, the dependence on  $f$  was not

tested since the model was compared only with experimental data for  $f = 4$ .

Polymer specific simulations on gelation that consider the coordinates of the molecules in space were pioneered by Leung and Eichinger<sup>114</sup>. The paper by Shy and Eichinger<sup>84</sup> uses this approach to estimate the position of the gel points. However, the data is not consistent as some gel points for large molecular weight lie below the Flory-Stockmayer prediction despite of a significant amount of intra-molecular reactions and the simulations do not enforce unequal reactivity. Also, the intra-molecular reactions show some unexpected trends (do not extrapolate towards zero for zero conversion; there is more cyclization for  $f = 4$  as compared to  $f = 3$  at low molecular weight but less at high molecular weight).

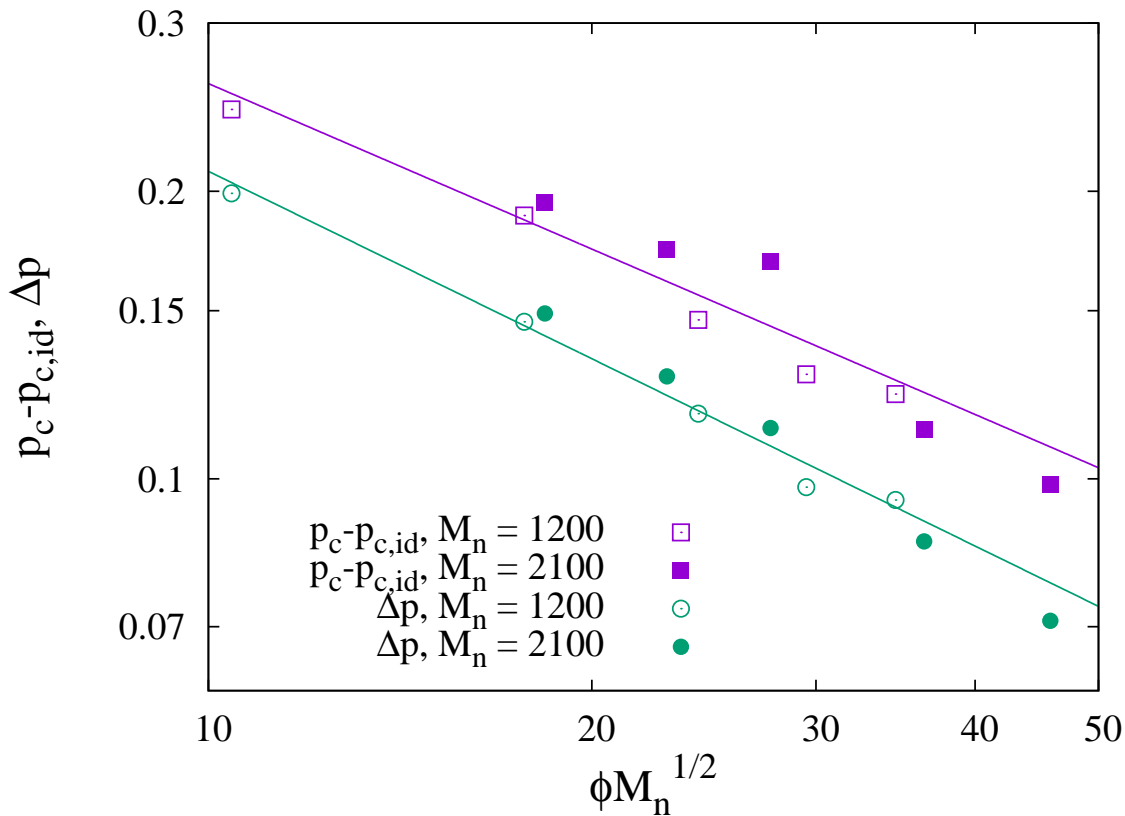


Figure 15: Simulation data of Ref.<sup>23</sup> for the shift of gel point  $p_{c,\text{sim}} - p_{c,\text{id}}$  and fraction of loops at the gel point,  $\Delta p$ .

In a subsequent work by Lee and Eichinger<sup>23</sup>, these apparent problems were resolved, however, the definition of conversion seems to be based upon the number of connections

between two polyoxypropylene tetrols through one hexamethylen diisocyanate as obvious from equation (8), the results for  $\lambda_{AB}$ , or the last two columns of table 3 in their paper (in effect  $p = q^2$  is used as “conversion” where  $q$  is the true conversion of reactive groups). With this conjecture, all of the presented data becomes self-consistent, agrees to the presented experimental data of Stepto’s group, and shows similar qualitative trends as the data of our work. It is discussed in Ref.<sup>23</sup> (independent of this conjecture) that the intra-molecular reactions are not sufficient to account for the shift of the gel point. Both, the shift of the gel point and the fraction of intra-molecular reactions are in accord with a power law decay as a function of the overlap of the molecules, see Figure 15. The corresponding exponents are  $-0.57 \pm 0.06$  and  $-0.65 \pm 0.03$  respectively, which are both smaller than  $\approx 2/3$  and  $-1.08 \pm 0.06$ , which were the corresponding exponents of our data, if plotted with the same axes and the same level of corrections as Figure 15.

Simulation data using the model of Ref.<sup>114</sup> was compared with experimental data of the Stepto group in Ref.<sup>25</sup>. This comparison yields reasonable predictions of gel points from simulation data, while mean field approaches underestimate systematically the gel point shift of experimental data.

Gupta et al.<sup>24</sup> introduce a long range percolation model but discuss it as a model for diffusion controlled reactions. The authors observe that cyclization accounts only for a part of the delay of the gel point. A subsequent work by Hendrickson et al.<sup>26</sup> uses an improved version of the original algorithm. Figure 6 of Ref.<sup>26</sup> shows that the shift in the conversion is significant and dominated by intra-molecular reactions for short range interactions, while for reactions with a longer range (larger overlap number), the spatial arrangement of the molecules becomes the dominant cause for the shift of the gel point. This latter contribution grows sublinear with the overlap number, which agrees qualitatively with our results. However, one has to be cautious regarding their results since the criterion used to determine the gel point does not reflect the true gel point of these systems. Another caveat regards the point that  $f$  decouples from node density in their simulations, while it does not for real

reactions in bulk, which leads to some counterintuitive results for the dependence on  $f$ .

Yang et al.<sup>28</sup> study network formation using Molecular Dynamics simulations. Apparently, not all of the presented data seem to be consistent and thus, need to be considered with care. Nevertheless, the measured gel points for  $N \geq 15$  at  $r = 1$  and  $\phi = 0.3$  are delayed by about 5-6 percent of conversion with respect to the mean field prediction of 0.707. However, the amount of intra-molecular reactions of these samples is only about 3% and thus, not sufficient to explain quantitatively the observed shift of the gel point.

Lang et al.<sup>36</sup> perform Monte-Carlo simulations of network formation and analyzed the loop size distribution. Here, exponents  $2.5 \pm 0.1$  and  $2.35 \pm 0.1$  were obtained in the vicinity of the presumed gel point for two series of data at different degree of dilution respectively. These exponents are in the same range as the data of Wang et al.<sup>22</sup> and more in line with mean field models as with percolation. In a later publication<sup>27</sup> by the same authors, it was recognized that intra-molecular reactions alone do not explain the shift between data and mean field theory in the vicinity of the gel point, see Figure 12 and 13 of Ref.<sup>27</sup> and the corresponding discussion.

## References

- (1) Samaddar, P.; Kumar, S.; Kim, K.-H. Polymer hydrogels and their applications toward sorptive removal of potential aqueous pollutants. *Polymer Reviews* **2019**, *39*, 418–464.
- (2) Farhood, B.; Geraily, G.; Abtahi, S. M. M. A systematic review of clinical applications of polymer gel dosimeters in radiotherapy. *Applied Radiation and Isotopes* **2019**, *143*, 47–59.
- (3) You, I.; Kong, M.; Jeong, U. Block copolymer elastomers for stretchable electronics. *Acc. Chem. Res.* **2019**, *52*, 63–72.

- (4) Qiu, Y.; Zhang, E.; Plamthottam, R.; Pei, Q. Dielectric elastomer artificial muscle: Materials innovations and device explorations. *Acc. Chem. Res.* **2019**, *52*, 316–325.
- (5) Flory, P. J. *Principles of polymer chemistry*; Cornell University Press, 1953.
- (6) Korolev, S. V.; Kuchanov, S. I.; Slin'ko, M. G. Calculation of gel points taking account of cyclization reactions. *Polymer Science U.S.S.R.* **1982**, *24*, 2489–2499.
- (7) van der Marck, S. C. Percolation thresholds and universal formulas. *Phys. Rev. E* **1997**, *55*, 1514–1517.
- (8) Rubinstein, M.; Colby, R. H. *Polymer Physics*; Oxford University Press, 2003.
- (9) Mertens, S.; Moore, C. Series expansion of the percolation threshold on hypercubic lattices. *J. Phys. A* **2018**, *51*, 475001.
- (10) Torquato, S.; Jiao, Y. Effect of dimensionality on the percolation thresholds of various d-dimensional lattices. *Phys. Rev. E* **2013**, *87*, 032149.
- (11) Flory, P. J. Molecular size distribution in three dimensional polymers. I. Gelation. *J. Am. Chem. Soc.* **1941**, *63*, 3083–3090.
- (12) Stockmayer, W. H. Theory of Molecular Size Distribution and Gel Formation in Branched-Chain Polymers. *J. Chem. Phys.* **1943**, *11*, 45–55.
- (13) Macosko, C. W.; Miller, D. R. A new derivation of average molecular weights of nonlinear polymers. *Macromolecules* **1976**, *9*, 199–206.
- (14) Miller, D. R.; Macosko, C. W. A new derivation of post gel properties of network polymers. *Macromolecules* **1976**, *9*, 206–211.
- (15) Harris, F. E. Ring formation and molecular weight distributions in branched-chain polymers. I. *J. Chem. Phys.* **1955**, *23*, 1518–1525.

- (16) Kilb, R. W. Dilute gelling systems. I. The effect of ring formation on gelation. *J. Chem. Phys.* **1958**, *62*, 969–971.
- (17) Ahmad, Z.; Stepto, R. F. T. Approximate theories of gelation. *Colloid and Polymer Science* **1980**, *258*, 663–674.
- (18) Suematsu, K. Theory of gel point in real polymer solutions. *Eur. Phys. J. B* **1998**, *6*, 93–100.
- (19) Sarmoria, C.; Miller, D. R. Spanning-tree models for  $A_f$  homopolymerizations with intramolecular reactions. *Comp. Theo. Pol. Sci.* **2001**, *11*, 113–127.
- (20) Suematsu, K. Recent progress in gel theory: Ring, excluded volume, and dimension. *Adv. Pol. Sci.* **2002**, *156*, 137–214.
- (21) Tanaka, Y.; Stanford, J. L.; Stepto, R. F. T. Interpretation of gel points of an epoxy-amine system including ring formation and unequal reactivity: reaction scheme and gel-point prediction. *Macromolecules* **2012**, *45*, 7186–7196.
- (22) Wang, R.; Lin, T.-S.; Johnson, J. A.; Olsen, B. D. Kinetic Monte Carlo Simulation for the quantification of the gel point of polymer networks. *ACS Macro Letters* **2017**, *4*, 1414–1419.
- (23) Lee, K.-J.; Eichinger, B. E. Computer simulation of the structure and elasticity of polyurethane networks: 1. Polyoxypropylene tetrols and hexamethylene diisocyanate. *Polymer* **1990**, *31*, 406–414.
- (24) Gupta, A. M.; Hendrickson, R. C.; Macosko, C. W. Monte Carlo description of  $A_f$  homopolymerization: Diffusional effects. *J. Chem. Phys.* **1991**, *95*, 2097–2108.
- (25) Dutton, S.; Rolfes, H.; Stepto, R. F. T. Comparison of Ahmad-Rolfes-Stepto theory, rate theory and Monte-Carlo modelling of gel point and network modulus. *Polymer* **1994**, *35*, 4521–4526.

- (26) Hendrickson, R. C.; Gupta, A. M.; Macosko, C. W. Monte Carlo simulation of cyclization during stepwise polymerization. *Comput. Pol. Sci.* **1995**, *5*, 135–142.
- (27) Lang, M.; Kreitmeier, S.; Göritz, D. Trapped entanglements in polymer networks. *Rubber Chemistry and Technology* **2007**, *80*, 873–894.
- (28) Yang, W.; Wei, D.; Jin, X.; Liao, Q. Molecular dynamics simulation of the formation of polymer networks. *Macromol. Theory Simul.* **2007**, *16*, 548–556.
- (29) Hoshen, J.; Kopelman, R.; Monberg, E. M. Percolation and cluster distribution. II. Layers, variable-range interactions, and exciton cluster model. *J. Stat. Phys.* **1978**, *19*, 219–242.
- (30) Stephen, M. J.; Aharony, A. Percolation with long-range interactions. *J. Phys. C* **1981**, *14*, 1665–1670.
- (31) Ord, G.; Whittington, S. G. Percolation on a randomly expanded lattice: A model of polymer gels. *J. Phys. A* **1982**, *15*, L29–L31.
- (32) Ray, T. S.; Klein, W. Crossover and the breakdown of hyperscaling in long-range bond percolation. *J. Stat. Phys.* **1988**, *53*, 773–794.
- (33) Meester, R.; Steif, J. E. On the continuity of the critical value for long range percolation in the exponential case. *Commun. Math. Phys.* **1996**, *180*, 483–504.
- (34) Frei, S.; Perkins, E. A lower bound for  $p_c$  in range-R bond percolation in two and three dimensions. *Electron. J. Probab.* **2016**, *21*, 1–22.
- (35) Aharony, A.; Stauffer, D. On the width of the critical region in dilute magnets with long range percolation. *Z. Phys. B. - Condensed Matter* **1982**, *47*, 175–177.
- (36) Lang, M.; Göritz, D.; Kreitmeier, S. Intramolecular reactions in randomly end-linked polymer networks and linear (co)polymerizations. *Macromolecules* **2005**, *38*, 2515–2523.

- (37) Sen, P.; Banerjee, K.; Biswas, T. Phase transitions in a network with a range-dependent connection probability. *Phys. Rev. E* **2002**, *66*, 037102.
- (38) Luijten, E.; Blöte, H. W. J. Boundary between long-range and short-range critical behavior in systems with algebraic interactions. *Phys. Rev. Lett.* **2002**, *89*, 025703.
- (39) Gaunt, D. S.; Guttmann, A. J.; Whittington, S. G. Percolation with restricted valence. *J. Phys. A* **1979**, *12*, 75–79.
- (40) Kertész, J.; Chakrabarti, B. K.; Duarte, J. A. M. S. Threshold and scaling in percolation with restricted valence. *J. Phys. A* **1982**, *15*, L13–L18.
- (41) Qian, X.; Deng, Y.; Liu, Y.; Guo, W.; Blöte, H. W. J. Equivalent-neighbor Potts models in two dimensions. *Phys. Rev. E* **2016**, *94*, 052103.
- (42) Ouyang, Y.; Deng, y.; Blöte, W. J. Equivalent-neighbor percolation models in two dimensions: Crossover between mean-field and short-range behavior. *Phys. Rev. E* **2018**, *98*, 062101.
- (43) Deng, Y.; Ouyang, Y.; Blöte, H. W. J. Medium-range percolation in two dimensions. *J. Physics Conf. Series* **2019**, *1163*, 012001.
- (44) Herrmann, H. J. Geometrical cluster growth models and kinetic gelation. *Phys. Rep.* **1986**, *136*, 153–227.
- (45) Meakin, P. Formation of fractal clusters and networks by irreversible diffusion-limited aggregation. *Phys. Rev. Lett.* **1983**, *51*, 1119–1122.
- (46) Lang, M. Cyclic structures in polymer model networks. *Macromol. Symp.* **2019**, *385*, 1800168.
- (47) Carmesin, I.; Kremer, K. The bond fluctuation method: a new effective algorithm for the dynamics of polymers in all spatial dimensions. *Macromolecules* **1988**, *21*, 2819–2823.



- (48) Deutsch, H. P.; Binder, K. Interdiffusion and self-diffusion in polymer mixtures: A Monte Carlo study. *J. Chem. Phys.* **1991**, *94*, 2294–2304.
- (49) Rabbel, H.; Breier, P.; Sommer, J.-U. Swelling behavior of single-chain polymer nanoparticles: Theory and simulation. *Macromolecules* **2017**, *50*, 7410–7418.
- (50) Lang, M.; Schuster, C.; Dockhorn, R.; Wengenmayr, M.; Sommer, J.-U. Testing the physics of knots with a Feringa nanoengine. *Phys. Rev. E* **2018**, *98*, 052501.
- (51) Müller, T.; Lang, M.; Sommer, J.-U. Tendomers - force sensitive bis-rotaxanes with jump-like deformation behavior. *Soft Matter* **2019**, *15*, 3671–3679.
- (52) Lang, M.; Fischer, J.; Sommer, J.-U. Effect of topology on the conformations of ring polymers. *Macromolecules* **2012**, *45*, 7642–7648.
- (53) Klos, J.; Sommer, J.-U. Dendrimer solutions: A Monte Carlo study. *Soft Matter* **2016**, *12*, 9007–9013.
- (54) Werner, M.; Sommer, J.-U. Translocation and induced permeability of random amphiphilic copolymers interacting with lipid bilayer membranes. *Biomacromolecules* **2014**, *16*, 125–135.
- (55) Kreer, T.; Baschnagel, J.; Müller, M.; Binder, K. Monte Carlo simulation of long chain polymer melts: Crossover from Rouse to reptation dynamics. *Macromolecules* **2001**, *34*, 1105–1117.
- (56) Meyer, H.; Wittmer, J. P.; Kreer, T.; Johner, A.; Baschnagel, J. Static properties of polymer melts in two dimensions. *J. Chem. Phys.* **2010**, *132*, 184904.
- (57) Lang, M. Monomer fluctuations and the distribution of residual bond orientations in polymer networks. *Macromolecules* **2013**, *46*, 9782–9797.

- (58) Lang, M.; John, A.; Sommer, J.-U. Model simulations on network formation and swelling as obtained from cross-linking co-polymerization reactions. *Polymer* **2016**, *82*, 138–155.
- (59) Paul, W.; Binder, K.; Heermann, D. W.; Kremer, K. Crossover scaling in semidilute polymer solutions: a Monte Carlo test. *Journal de Physique II* **1991**, *1*, 37–60.
- (60) Wittmer, J. P.; Beckrich, P.; Meyer, H.; Cavallo, A.; Johner, A.; Baschnagel, J. Intramolecular long-range correlations in polymer melts: The segmental size distribution and its moments. *Physical Review E - Statistical, Nonlinear, and Soft Matter Physics* **2007**, *76*, 1–18.
- (61) Lang, M.; Michalke, W.; Kreitmeier, S. Optimized decomposition of simulated polymer networks into meshes. *Macromol. Theory Simul.* **2001**, *10*, 204–208.
- (62) Dušek, K.; Gordon, M.; Ross-Murphy, S. B. Graphlike state of matter. 10. Cyclization and concentration of elastically active network chains in polymer networks. *Macromolecules* **1978**, *11*, 236–245.
- (63) Hoffmann, M.; Lang, M.; Sommer, J.-U. Gelation threshold of cross-linked polymer brushes. *Phys. Rev. E* **2011**, *83*, 021803.
- (64) Colby, R. H.; Rubinstein, M.; Gillmor, J. R.; Mourey, T. H. Scaling properties of branched polyesters. 2. Static scaling above the gel point. *Macromolecules* **1992**, *25*, 7180–7187.
- (65) Rubinstein, M.; Colby, R. H. Elastic modulus and equilibrium swelling of near-critical gels. *Macromolecules* **1994**, *27*, 3184–3190.
- (66) Gusev, A. A. Numerical estimates of the topological effects in the elasticity of Gaussian polymer networks and their exact theoretical description. *Macromolecules* **2019**, *52*, 3244–3251.

- (67) Zhong, M.; Wang, R.; Kawamoto, K.; Olsen, B. D.; Johnson, J. A. Quantifying the impact of molecular defects on polymer network elasticity. *Science* **2016**, *353*, 1264–1268.
- (68) Lang, M. On the elasticity of phantom model networks with cyclic defects. *ACS Macro Letters* **2018**, *7*, 536–539.
- (69) Panyukov, S. P. Loops in polymer networks. *Macromolecules* **2019**, *52*, 4145–4153.
- (70) Lang, M. On the elasticity of polymer model networks containing finite loops. *Macromolecules* **2019**, *52*, 6266–6273.
- (71) Obukhov, S. P.; Rubinstein, M.; Colby, R. H. Network modulus and superelasticity. *Macromolecules* **1994**, *27*, 3191–3198.
- (72) Gordon, M. Network theory of rubber elasticity. *Proc. Int. Rubber Conference, Moscow ("Khimiya")* **1971**,
- (73) Skal, A. S.; Shklovskii, B. I. Topology of an infinite cluster in the theory of percolation and its relationship to the theory of hopping conduction. *Sov. Phys. Semiconduct.* **1975**, *8*, 1029–1032.
- (74) De Gennes, P. G. On a relation between percolation theory and the elasticity of gels. *Journal de Physique Lett.* **1976**, *37*, L1–L2.
- (75) Sahimi, M. Non-linear and non-local transport processes in heterogeneous media: from long-range correlated percolation to fracture and materials breakdown. *Physics Reports* **1998**, *306*, 213–395.
- (76) Isichenko, M. B. Percolation, statistical topography, and transport in random media. *J. Chem. Phys.* **2014**, *141*, 104902.
- (77) Stenull, O.; Hansen, G. K.; Oerding, K. Critical exponents for diluted resistor networks. *Phys. Rev. E* **1999**, *59*, 4919–4930.

- (78) Sahimi, M.; Hughes, B. D.; Scriven, L. E.; Davis, H. T. Critical exponent of percolation conductivity by finite-size scaling. *J. Phys. C* **1983**, *16*, L521–L527.
- (79) Gingold, D. B.; Lobb, C. J. Percolative conduction in three dimensions. *Phys. Rev. B* **1990**, *42*, 8220–8224.
- (80) de Alcantara Bonfim, O. F.; Kirkham, J. E.; McKane, A.-J. Critical exponents for the percolation problem and the Yang-Lee edge singularity. *J. Phys. A*. **1981**, *14*, 2391–2413.
- (81) Adler, J.; Meir, Y.; Aharony, A.; Harris, A. B. Series study of percolation moments in general dimension. *Phys. Rev. B*. **1990**, *41*, 9183–9206.
- (82) Strenski, P. N.; Bradley, R. M.; Debierre, J.-M. Scaling behavior of percolation surfaces in three dimensions. *Phys. Rev. Lett.* **1991**, *66*, 1330–1333.
- (83) Stauffer, D.; Coniglio, A.; Adam, M. Gelation and Critical Phenomena. *Advances in Polymer Science* **1982**, *44*, 103–158.
- (84) Shy, L. Y.; Leung, Y. K.; Eichinger, B. E. Critical exponents for off-lattice gelation of polymer chains. *Macromolecules* **1985**, *18*, 983–986.
- (85) Cheng, K.-C.; Chiu, W.-Y. Monte Carlo simulation of polymer network formation with complex chemical reaction mechanism: kinetic approach on Curing of Epoxides with Amines. *Macromolecules* **1994**, *27*, 3406–3414.
- (86) Cail, J. I.; Stepto, R. F. T.; Taylor, D. J. R. Formation, structure and properties of polymer networks: Gel-point prediction in endlinking polymerisations. *Macromol. Symp.* **2001**, *171*, 19–36.
- (87) Rolfes, H.; Stepto, R. F. T. A development of Ahmad-Stepto gelation theory. *Makromol. Chem. - Macromol. Symp.* **1993**, *76*, 1–12.

- (88) Cail, J. I.; Stepto, R. F. T. The gel point and network formation - theory and experiment. *Polymer Bull.* **2007**, *58*, 15–25.
- (89) Lang, M.; Rubinstein, M.; Sommer, J.-U. Conformations of a long polymer in a melt of shorter chains: Generalizations of the Flory theorem. *ACS Macro Letters* **2015**, *4*, 177–181.
- (90) Zhou, H.; Woo, J.; Cok, A. M.; Wang, M.; Olsen, B. D.; Johnson, J. A. Counting primary loops in polymer gels. *PNAS* **2012**, *109*, 19119–19124.
- (91) Gordon, M.; Scantlebury, G. R. Statistical kinetics of polyesterification of adipic acid with pentaerythritol or trimethylol ethane. *J. Chem. Soc. B* **1967**, 1–13.
- (92) Spouge, J. L. Equilibrium ring formation in polymer solutions. *J. Stat. Phys.* **1986**, *43*, 143–196.
- (93) Tanaka, Y.; Stanford, J. L.; Stepto, R. F. T. Interpretation of gel points of an epoxy-amine system including ring formation and unequal reactivity: Measurements of gel points and analyses of ring structures. *Macromolecules* **2012**, *45*, 7197–7205.
- (94) Nishi, K.; Fujii, K.; Chung, U.-I.; Shibayama, M.; Sakai, T. Experimental observation of two features unexpected from the classical theories of rubber elasticity. *Phys. Rev. Lett.* **2017**, *119*, 267801.
- (95) Semenov, A. N. Theory of long-range interactions in polymer systems. *J. Phys. II France* **1996**, *6*, 1759–1780.
- (96) Deng, Y. *Private communication*.
- (97) de Gennes, P.-G. *De Gennes - Scaling concepts in polymer physics*; Cornell University Press: Ithaca and London, 1979.
- (98) Stanford, J. L.; Stepto, R. F. T. A Study of intramolecular reaction and gelation during non-linear polyurethane formation. *Brit. Polym. J* **1977**, *9*, 124–132.

- (99) Matějka, L.; Dušek, K. Formation of polyurethane networks studied by the gel point method. *Polymer Bull.* **1980**, *3*, 489–495.
- (100) Ďuračková, A.; Valentová, H.; Dušková-Smrčková, M.; Dušek, K. Effect of diluent on the gel point and mechanical properties of polyurethane networks. *Polymer Bull.* **2007**, *58*, 201–211.
- (101) Zhao, D.; Liao, G.; Gao, G.; Liu, F. Influences of intramolecular cyclization on structure and cross-linking reaction processes of PVA hydrogels. *Macromolecules* **2006**, *39*, 1160–1164.
- (102) Dušková-Smrčková, M.; Valentová, H.; Ďuračková, A.; Dušek, K. Effect of dilution on structure and properties of polyurethane networks. Pregel and postgel cyclization and phase separation. *Macromolecules* **2010**, *43*, 6450–6462.
- (103) Stepto, R. F. T. Theoretical and experimental studies of network formation and properties. *Polymer* **1979**, *20*, 1324–1326.
- (104) Stepto, R. F. T. Formation and properties of polymer networks. *Acta Polymerica* **1988**, *39*, 61–66.
- (105) Stepto, R. F. T.; Cail, J. I.; Taylor, D. J. R. Predicting the formation, structure and elastomeric properties of end-linked polymer networks. *Macromol. Symp.* **2000**, *159*, 163–178.
- (106) Stepto, R. F. T.; Taylor, D. J. R.; Partchuk, T.; Gottlieb, M. Poly(dimethylsiloxane) gelation studies. *ACS Symposium Series* **2000**, *729*, 194–203.
- (107) Wile, L. L. Ph.D. thesis, 1945.
- (108) Šomvářsky, J.; Dušek, K. Kinetic Monte-Carlo simulation of network formation. I. Simulation method. *Polymer Bulletin* **1994**, *33*, 369–376.

- (109) Šomvářsky, J.; Dušek, K. Kinetic Monte-Carlo simulation of network formation. II. Effects of system size. *Polymer Bull.* **1994**, *33*, 377–384.
- (110) Šomvářsky, J.; Dušek, K.; Smrčková, M. Kinetic modelling of network formation: Size-dependent static effects. *Comp. Theo. Polym. Sci.* **1998**, *8*, 201–208.
- (111) Sarmoria, C.; Valles, E.; Miller, D. R. Ring-chain competition kinetic models for linear and nonlinear step-reaction copolymerizations. *Macromol. Chem. Macromol. Symp.* **1986**, *2*, 69–87.
- (112) Rankin, S. E.; Kasehagen, L. J.; McCormick, A. V.; Macosko, C. W. Dynamic Monte Carlo simulation of gelation with extensive cyclization. *Macromolecules* **2000**, *33*, 7639–7648.
- (113) Pereda, S.; Brandolin, A.; M., V. E.; Sarmoria, C. Copolymerization between  $A_3$  and  $B_2$  with ring formation and different intrinsic reactivity in one of the Monomers. *Macromolecules* **2001**, *34*, 4390–4400.
- (114) Leung, Y. K.; Eichinger, B. E. Computer simulation of end-linked elastomers. I. Tri-functional networks cured in the bulk. *J. Chem. Phys.* **1984**, *80*, 3877–3884.

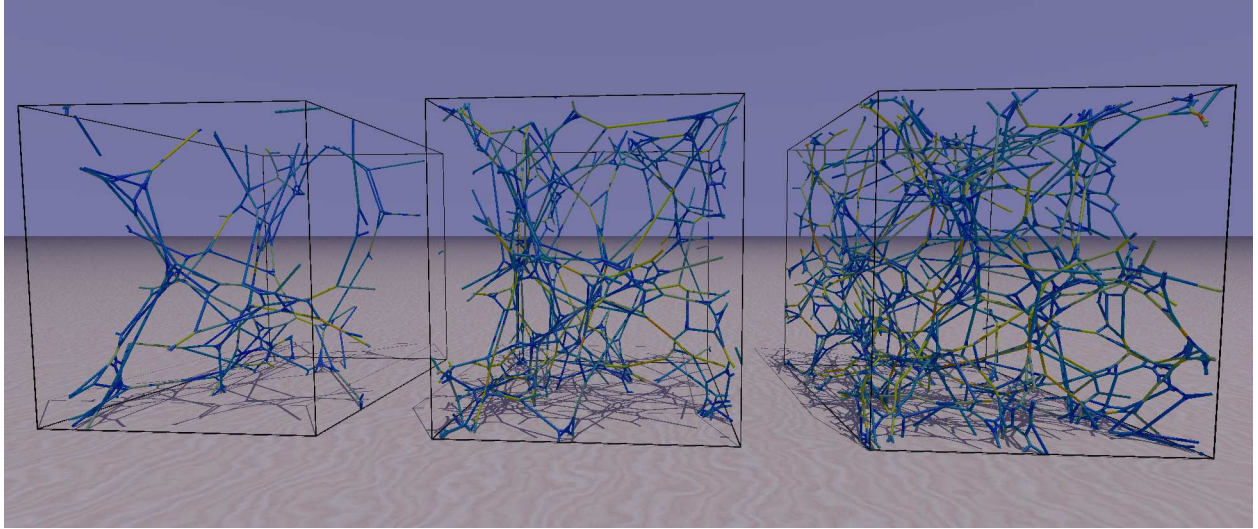


Table of Contents Graphics: The force balance condition for the determination of the phantom modulus of a network with junction functionality  $f = 4$  and chain degree of polymerization  $N = 8$  is shown at three different conversions  $p = 0.66, 0.67,$  and  $0.68$  not far beyond the gel point.



This figure "Figure1.png" is available in "png" format from:

<http://arxiv.org/ps/2104.05257v1>

This figure "TOC.png" is available in "png" format from:

<http://arxiv.org/ps/2104.05257v1>